1987Metic..22...25K

LATE EOCENE IMPACT MICROSPHERULES: STRATIGRAPHY, AGE AND GEOCHEMISTRY

G. Keller and S.L. D'Hondt
Department of Geological and Geophysical Sciences
Princeton University
Princeton, NJ 08544

C.J. Orth, J.S. Gilmore, and P.Q. Oliver
Los Alamos National Laboratory
Los Alamos, NM 87545

E.M. Shoemaker
U.S. Geological Survey
Flagstaff, AZ 08001

E. Molina
Departmento de Paleontologia
Universidad de Zaragoza
50009-Zaragoza, España

Recent discoveries of microtektite and related crystal bearing microspherule layers in deep-sea sediments of the west equatorial Pacific DSDP Sites 292, 315A and 462, off-shore New Jersey in Site 612 and in southern Spain have confirmed the presence of at least three microspherule layers in Late Eocene sediments. Moreover, these discoveries have extended the North American strewn field from the Caribbean and Gulf of Mexico region to the northwest Atlantic, and have established a third strewn field in western equatorial Pacific and Indian Ocean which may extend to the Mediterranean.

Stratigraphically the oldest microspherule layer occurs in the planktonic foraminifer Globigerapsis semiinvoluta *Zone about 0.5 m.y. prior to the closely spaced crystal bearing microspherule layer and North American microtektite layer in the* Globorotalia cerroazulensis *Zone. Major element composition of the* G. semiinvoluta *Zone layer and the crystal bearing microspherule layer overlap, but there is a clear trend towards higher* Al_2O_3 *and FeO values in* SiO_2 *equivalent microspherules of the latter layer. The* G. semiinvoluta *Zone microspherules also contain a higher percentage of non-crystalline spherules (microtektites) than the crystal bearing microspherule layer, but lower than the North American microtektite layer. Excess iridium due to an abrupt increase in supply is associated with the middle crystal bearing microspherule layer and to a lesser extent with the other two layers. But, Ir excess due to concentration as a result of carbonate loss was also observed at two sites (462, 612).*

The three late Eocene microspherule layers do not precisely coincide with planktonic foraminiferal species extinctions, but a major faunal assemblage change is associated with the G. semiinvoluta *Zone layer. Abundant pyrite is present in the North American microtektite layer of DSDP Site 612 suggesting reducing conditions possibly due to a sudden influx of biologic matter*

© Meteoritical Society • Provided by the NASA Astrophysics Data System

1987Metic..22...25K

(dead bodies) to the ocean floor, and the crystal bearing microspherule layer coincides with five radiolarian extinctions. All three microspherule layers are associated with decreased carbonate possibly due to sudden productivity changes, increased dissolution as a result of sea-level and climate fluctuations, or the impact events.

INTRODUCTION

Most workers now believe that macrotektites and microtektites are the product of dispersion of predominantly terrestrial target rock resulting from the impact of an extraterrestrial body (Taylor, 1973; King, 1977; Glass *et al.*, 1979, 1982; Ngo *et al.*, 1985). But regardless of the origin of microtektites, two main questions arise with their presence in late Eocene sediments. Firstly, do impact events cause mass extinctions of biota similar to those observed at the Cretaceous-Tertiary boundary, and/or trigger long-term environmental or climatic changes with major consequences for life on Earth? And secondly, is there evidence of multiple microtektite layers or impact events in late Eocene sediments (Keller *et al.*, 1983; Glass *et al.*, 1985) which would suggest that the Earth encountered a swarm of comets (Hut *et al.*, in press).

Currently, the only documented case of a global mass extinction associated with, and most likely triggered by a large body Earth impact is at the Cretaceous-Tertiary boundary (65 million years ago). In view of recent reports of a 26 to 33 million year periodicity in extinction events (Raup and Sepkoski, 1984), and of a similar periodicity in the age distribution of terrestrial impact craters (Rampino and Stothers, 1984), it is important to search for good physical, chemical and biological (fossil) evidence of events similar to that at the Cretaceous-Tertiary boundary, but elsewhere in the geologic column. Late Eocene marine sediments with recognized microtektite and associated crystal bearing microspherule layers and good microfossil control provide an excellent opportunity to test the hypothesized relationship between mass extinctions and impact events.

Previous studies have shown that mass extinctions are episodes of accelerated loss of taxa generally occurring stepwise over a period of several million years (Kauffman, 1984; Keller, 1986a, b). The late middle Eocene through late Eocene time represents such a mass extinction episode characterized by four steps of accelerated loss of taxa among planktonic foraminifera (Keller, 1986a, b). None of these stepwise extinctions coincides precisely with the microtektite or microspherule layers. The oldest *Globigerapsis semiinvoluta* Zone layer is associated with the decline of the *Globigerapsis* group and their extinction, which marks one of the steps, occurs shortly above this layer. The second crystal bearing microspherule layer in the *Globorotalia cerroazulensis* Zone and near the radiolarian *Calocyclas bandyca/Cryptopora ornata* Subzone boundary, is associated with the extinction of four radiolarian species (Maurasse and Glass, 1974; Sanfilippo *et al.*, 1985), but no species extinctions among planktonic foraminifera. The third microtektite layer in the *Gl. cerroazulensis* Zone represented by the North American layer appears to be associated with a major population shift of ecologically sensitive planktonic foraminiferal species noted especially in DSDP Site 612. The principle extinction event of the four stepwise extinctions occurs at the middle/late Eocene boundary about 0.5 million years prior to the first of the three late Eocene microtektite and microspherule layers.

© Meteoritical Society • Provided by the NASA Astrophysics Data System

1987Metic..22...25K

Microtektites (non-crystalline microspherules), and related crystal bearing microspherules are generally indistinguishable to the naked eye, but the latter contain microlites when viewed in thin sections. Both types of microspherules are generally spherical although a few dumbbell or teardrop shapes can be found. They range in color from milky opaque to yellow, brown, and black. Both types of microspherules have been observed in all three Late Eocene microspherule layers although in highly variable proportions. The youngest, or North American microtektite layer, contains only about 2-6% crystal bearing microspherules, the middle layer contains 68-72% and is known as the crystal bearing microspherule layer (Glass *et al.*, 1985), and the oldest *Globigerapsis semiinvoluta* Zone layer has a mixture of both with 18% crystal bearing microspherules. In this paper we will follow the convention and restrict the term "microtektite" layer to the youngest (North American) strewn field because of their predominance of non-crystalline spherules. The two older layers will be referred to as microspherule layers.

Microspherules of the uppermost layer, the North American microtektite layer have been found in the Caribbean, Gulf of Mexico and Western North Atlantic (Fig. 1). The second layer with abundant crystal bearing spherules has been found in the equatorial Pacific, Caribbean and Gulf of Mexico (Glass *et al.*, 1979, 1985). The third and oldest layer in the *G. semiinvoluta* Zone has been found in the Western equatorial Pacific and eastern Indian Ocean. Recently microspherules have also been found at this stratigraphic horizon in southern Spain, but their chemistry is significantly different from microspherules of the same horizon in the equatorial region (Fig. 1).

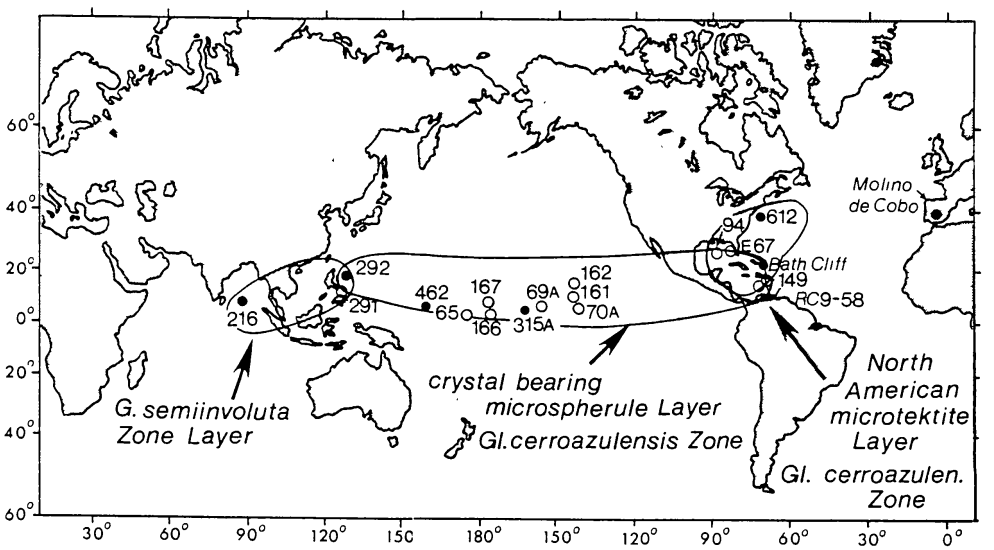

Fig. 1 Geographic distribution of DSDP sites and other localities where Late Eocene microtektites and crystal-bearing microspherules of three stratigraphic horizons have been found. Black circles mark localities discussed in this report. Locality and stratigraphic data of all sites are listed in Table 1.

© Meteoritical Society • Provided by the NASA Astrophysics Data System

1987Metic..22...25K

We report here on the stratigraphy, faunal changes and geochemistry of sediments in terms of $CaCO_3$, Ir and stable isotopes, associated with the Late Eocene microtektite and microspherule layers. Microprobe analysis of major element compositions of microspherules show that there is some compositional overlap in all three Late Eocene layers as well as with the Pleistocene Australasian and Ivory Coast microtektites, but multivariate statistical analysis permits identification of three Late Eocene microspherule layers (D'Hondt *et al.*, 1987).

PROCEDURES

The stratigraphy of late Eocene sections was determined from routine first and last appearances of index species as well as quantitative faunal analysis to provide high resolution stratigraphic control and paleoceanographic and paleoclimatic information (Keller, 1983, 1986a). Near critical faunal changes and microspherule layers samples were analyzed at approximately 15-20 cm intervals and microspherules were picked for geochemical analysis (D'Hondt *et al.*, 1987). Frequently, however, those intervals were nearly depleted in the working halves of the DSDP cores and in some cases the precise location of the loose remaining core sediment could not be determined with certainty. The stratigraphic position of microspherule layers was therefore determined also from the undisturbed archive cores using a binocular microscope. This method permitted precise determination of the location and maximum concentration of microspherule layers and their dispersal above and below due to bioturbation (Table 1). The peak in the distribution of microtektites and microspherules, assumed to represent the time of impact, usually did not exceed 2 to 5 cm. Bioturbation generally resulted in dispersal of some microspherules to 25 cm above and below the layer, and in some cases to $\pm$ 50 cm. With meticulous searching we could "home-in" on the peaks. The stratigraphic occurrence of microspherule layers is shown in Table 1 along with the number of microspherules found. For DSDP Site 612 the weight percent microtektites and tektite debris in the size fraction > 63 μm was calculated by separating them from the residue. Samples for Ir analysis were dried, pulverized, and irradiated with thermal neutrons in the Los Alamos Omega West Reactor. After several days decay of shorter-lived radionuclides, the irradiated samples were dissolved and Ir was isolated by radiochemical methods. Details are given in Orth *et al.* (1982). Carbonate content was determined with a CO_2 coulometer carbon analyzer to an accuracy of $\pm$ 0.5%.

To assess whether impact events are associated with climatic changes, stable isotopes of individual planktonic and benthonic foraminiferal species were analyzed by Lloyd Keigwin of Woods Hole Oceanographic Institute. The results are inconclusive (Table 2). Generally, isotope values are highly variable suggesting rapidly fluctuating temperature conditions, postdepositional diagenetic alteration of carbonate tests, and/or vital effects. For these reasons, our data show no consistent climatic signal associated with the microspherule layers.

© Meteoritical Society • Provided by the NASA Astrophysics Data System

1987Metic..22...25K

Table 1

Stratigraphic occurrence of microspherule layers. Stratigraphic position of maximum concentration of layer and dispersal due to bioturbation determined by Core sample analysis and examination of the archive cores. Number of microspherules refers to actual number observed in a sediment sample of about 5 cubic centimeter. 'A' marks presence of a large number of microspherules that has not been counted. At DSDP Site 612 microtektites constitute 50% by weight of the sediment fraction > 63 μm. The radiolarian Subzone b/c of T. bromia Zone refers to *C. bandyca/C. ornata*.

DSDP SITE	*Microspherule Layer Core-Section (cm)*		*Number of microspherules*	*Stratigraphic Zone*
	max. concentration	*bioturbation*	*A = abundant*	
69A	9-5(28-42)	9-5(12-50)	83	T.bromia, b/c
70A	27-3(28-30)	27-3(20-37)	6	T.bromia, b/c
94	15-4(40-42)	15-4(0-90)	44	T.bromia, b/c Gl. cerroazulensis
149	31-1(0-10)	31-1(0-51)	22	T.bromia, b/c
166	12-6(65-72)	12-6(41-93)	1400/gm[1]	T.bromia, b/c
167	28-1(36-38)	28-1(5-62)	43	T.bromia, b/c Gl. cerroazulensis
216	16-1(145)-16-2(5)	16-1(140)-16-2(15)	3400/gm[1]	T.bromia, b/c G. semiinvoluta
291	4-2(40-120)		3	T.bromia
292		36-2(70-130)	4	T.bromia, c Gl. cerroazulensis
292		36-4	6	T.bromia, b/c Gl. cerroazulensis
292	38-2(75-80)	38-2(35-90)	31	G. semiinvoluta
315A	10-6(43-47)	10-5(27)-10-6(50)	174	T.bromia, NP20/21
462	36-1(145)-36-2(7)	36-1(134)-36-2(108)	A	T.bromia, Gl. cerroazulensis
612	21-5(115-117)	none	A*	T.bromia, b/c, Gl. cerroazulensis
E67	5198 ft		8	Gl. cerroazulensis
E67	5209-5213 ft		5[x]	G. semiinvoluta
RC9-58	254 cm		2800/gm[1]	T.bromia
RC9-58	280 cm		3000/gm[1]	T.bromia
Barbados	0-8 cm		A	T.bromia, b/c, Gl. cerroazlensis
SPAIN, Molino de Cobo			21	G. semiinvoluta

[1] From Glass *et al.* (1985)

A* microtektites are 50% by weight of sediment fraction > 63 μm

[x] these microspherules may be due to downcore contamination

b/c denotes Radiolarian Subzone C. bandyca/C. ornata

© Meteoritical Society • Provided by the NASA Astrophysics Data System

1987Metic..22...25K

Table 2

Carbonate, iridium, oxygen and carbon isotope data of planktonic foraminifer *Globigerina galavisi* (Site 292) and benthonic foraminifer *Cibicidoides* (Sites 315A, 216), for DSDP Sites 292, 462, 315A, 216, 612 and Barbados.

Core-Section (cm) Site 292	$CaCO_3$ (%)	^{18}O	^{13}C (PDB)	Ir (ppt)
29-1 (99-101)	88.29			
29-1 (118-120)	93.77			
29-1 (141-143)	88.12			
29 cc	81.97			
30-1 (63-65)	90.14			
30-1 (86-88)	95.53			
30-1 (139-141)	91.23			
30-2 (88-90)	91.81			
30-2 (109-111)	95.97			
30-2 (138-140)	86.81			
36-1 (70-72)	85.89	−0.60	1.88	20
36-1 (108-110)	85.52	−0.92	1.82	
36-1 (135-137)	80.88	−0.92	2.00	
36-2 (34-36)	80.52	−0.81	1.91	
36-2 (43-45)	82.37	−0.89	1.81	
36-2 (58-61)	80.84	−0.95	1.90	19
36-2 (70-72)	72.83	−0.76	1.87	22
36-2 (99-100)	74.71	−0.90	1.86	26
36-2 (130-133)	77.89	−0.90	1.83	24
36-2 (143-145)	80.88	−0.93	1.91	18
36-3 (20-22)	86.97	−0.99	2.10	25
36-3 (40-42)		−0.99	1.76	
36-3 (66-68)	88.55	−0.86	1.60	17
36-3 (100-102)	77.26	−0.75	1.62	19
36-3 (130-132)		−1.02	1.87	
36-4 (0-2)	70.06	−1.08	1.84	19
36-4 (37-39)	40.62			29
36-4 (70-72)		−0.78	1.76	
36-4 (113-115)	84.67	−0.76	1.87	29
36-5 (28-30)	82.34	−0.75	1.82	
36-5 (57-59)		−0.66	1.93	
36-5 (64-66)	83.72			19
36-5 (135-137)	81.09			
36 cc		−0.94	1.86	
37-1 (98-100)	79.11			
37-1 (128-130)	78.44	−0.67	1.83	
37-1 (143-145)	80.69	−0.86	1.87	
37-2 (26-28)	87.30			13
37-2 (53-55)	79.11			
37-2 (130-132)	85.85	−0.97	1.86	
37-3 (22-24)	78.22			20
37-3 (50-52)		−0.86	2.01	
37-3 (99-101)	82.35	−0.65	1.89	15

© Meteoritical Society • Provided by the NASA Astrophysics Data System

1987Metic..22...25K

Table 2 continued

Core-Section (cm) Site 292	$CaCO_3$ (%)	^{18}O	^{13}C (PDB)	Ir (ppt)
37-3 (99-101) duplicate		−0.93	2.02	
37-3 (121-123)	80.69	−0.67	2.01	17
38-1 (145-147)	75.60	−0.75	2.16	29
38-2 (1-2)	75.72	−0.63	2.00	32
38-2 (1-2) duplicate		−0.46	2.12	
38-2 (19-21)	63.73	−0.46	2.21	51
38-2 (19-21) duplicate		−0.77	2.12	
38-2 (35-37)	73.31	−0.02	1.88	
38-2 (35-37) duplicate		−0.25	2.04	
38-2 (35-37) duplicate		−0.34	1.85	
38-2 (35-37) duplicate		−0.64	2.15	
38-2 (35-37) duplicate		−0.43	2.21	
38-2 (50-52)	61.40	−0.70	2.12	40
38-2 (69-71)	43.46		2.12	40
38-2 (84-85)		−0.43	2.01	
38-2 (84-85) duplicate		−0.60	2.24	
38-2 (110-114)	87.43	−0.64	2.00	17
38-2 (110-114) duplicate		−0.74	2.12	
38-2 (131-133)		−0.84	2.12	
38-2 (141-143)	88.21	−0.42	1.66	20
39-1 (89-91)		−0.42	1.06	
Site 315A				
10-5 (44-46)	15.33	0.49	1.03	89
10-5 (106-107)	22.80	0.75	0.97	76
10-6 (11-13)	0.00			76
10-6 (25-27)	44.53	0.17	1.09	140
10-6 (38-40)	26.27	0.38	1.12	250
10-6 (54-57)	15.48	−0.15	1.25	140
10-6 (73-75)	5.01	−0.01	0.98	96
10-6 (73-75) duplicate	3.86			
10-6 (100-103)	8.60	−0.07	1.26	71
Site 216				
16-1 (70-72)	95.59	0.84	1.43	
16-1 (111-113)	92.11			
16-1 (127-129)	88.16	0.97	1.18	
16-1 (130-132)	88.31			
16-2 (1-5)	83.59	0.48	1.14	
16-2 (26-28)	84.08	0.61	1.11	
16-2 (43-46)	86.54			
16-2 (60-62)	84.97	0.37	1.26	
16-2 (81-83)	96.23	0.33	1.18	
16-2 (95-97)	98.54	0.64	1.32	
16-2 (125-127)	87.95	0.28	1.10	
16-3 (38-40)		0.48	1.19	
16-3 (60-63)		0.69	1.31	
17-1 (72-76)		0.45	0.95	
17-2 (60-62)		0.57	0.85	

© Meteoritical Society • Provided by the NASA Astrophysics Data System

1987Metic..22...25K

Table 2 continued

Core-Section (cm) Site 462	$CaCO_3$ (%)	Ir (ppt)	Bath Cliff	Ir (ppt)
34-1 (58-60)	78.72		EO-98	43
34-1 (58-60) duplicate	78.13		EO-97	50
35-1 (32-34)	90.98	18	EO-96	58
35-1 (50-52)		54	EO-95	58
36-1 (25-27)	74.83		EO-94	55
36-1 (25-27) duplicate	46.56		EO-92	50
"	47.41		EO-90	51
"	69.79			
36-1 (50-52)	54.73		EO-86	47
36-1 (99-101)	76.74	120	EO-85	54
36-1 (99-101) duplicate	74.88		EO-84	40
36-1 (125-127)	18.98	160	EO-83	32
36-1 (136-138)	7.32	220	EO-82	35
36-1 (144-146)	6.69	210	EO-81	56
36-2 (5-7)	10.17			
36-2 (5-7) duplicate	12.02		EO-80	46
36-2 (25-27)	1.25		EO-79	41
36-2 (50-52)	22.38	180	EO-77	35
36-2 (77-79)	45.49		EO-76	36
36-2 (77-79) duplicate	44.27		EO-45(EMS-27)	60
"	35.80		EO-44	41
"	33.86		EO-75(EO-43)	47
36-2 (79-81)	71.67	32	EO-74(EO-42)	38
36-2 (79-81) duplicate	83.91		EO-72(EO-40)	51
"	84.08		EO-71(EO-39)	41
36-2 (97-99)	3.27	68	EO-70(EO-38)	40
36-2 (97-99) duplicate	4.13		EO-69(EO-37)	52
"	0.26		EO-68(EO-36)	
36-2 (130-132)	43.78	79	EO-67(EO-35)	47
36-2 (130-132) duplicate	48.56		EO-66(EO-34)	54
"	44.12		EO-65	31
36-3 (25-27)	78.10		EO-64	57
36-3 (50-52)	83.17		EO-63	51
36-3 (75-77)	83.25		EO-62	25
36-3 (75-77) duplicate	84.12		EO-61	26
36-4 (6-8)	82.71		EO-60	32
36-4 (25-27)	84.46		EO-58	43
36-4 (58-60)	2.49		EO-57	41
36-4 (58-60) duplicate	2.76		(EO-33)	46
"	2.44		(EO-31)	48
"	0.50		(EO-30)	45
"	0.86		(EO-28)	38
"	0.48		(EO-26)	43
37-1 (25-27)	78.33		EO-56	41
37-1 (50-52)	80.44		EO-54	35
37-1 (75-77)	74.24		EO-52	41

© Meteoritical Society • Provided by the NASA Astrophysics Data System

1987Metic..22...25K

Table 2 continued

Core-Section (cm) Site 462	$CaCO_3$ (%)	Ir (ppt)	Bath Cliff	Ir (ppt)
37-1 (100-102)	77.01		EO-50	28
37-1 (125-127)	78.04		EO-49	28
37-1 (125-127) duplicate	77.86		EO-48	31
37-2 (25-27)	77.04		EO-47	48
37-2 (50-52)	78.56		EO-46	34
37-2 (75-77)	80.44		EO-16	63
37-2 (108-110)	76.27		EO-12	81
37-2 (146-148)	68.64		EO-11	85
			EO-10	87
SITE 612			EO-9	103
			EO-8	116
21-5 (54-55)	34.61	37	EO-7	97
21-5 (79-80)	34.62		EO-6	117
21-5 (86-87)	33.20	39	EO-5	140
21-5 (95-96)	29.53	59	EO-4	292
21-5 (101-102)	21.33	104	EO-3	40
21-5 (107-108)	32.92	60	EO-2	65
21-5 (113-114)	8.40	52	EO-1	33
21-5 (117-118)	22.04	16		
21-5 (132-133)	44.53	12		
21-5 (139-140)	46.07	10		
21-6 (11-13)	44.60			
21-6 (38-40)	54.91	9		
21-6 (66-68)	48.70			
21-6 (90-92)	52.68	10		

AGE DETERMINATION

The age of the Eocene-Oligocene boundary is still controversial. It appears that this boundary is probably younger than 36.5 Ma and that the late Eocene interval is also considerably shorter than previously accepted (Ness *et al.*, 1980; Harland *et al.*, 1982; Lowrie *et al.*, 1982; Hsu *et al.*, 1984; Berggren *et al.*, 1985). Recently, Montaneri *et al.* (1985) estimated an age of 35.7 ± 0.4 Ma for the Eocene-Oligocene boundary based on five upper Eocene and lower Oligocene K/Ar and Rb/Sr dates of volcanic biotites. Their Oligocene ages are essentially in agreement with published time scales, but their late Eocene ages are surprisingly young. They obtained an age of 36.0 ± 0.4 Ma for the uppermost part of the *Globigerapsis semiinvoluta* Zone and 36.4 ± 0.4 Ma for the lower part of this zone. If their ages are correct, then the late Eocene is represented by a very short time interval of 0.7 ± 0.4 m.y. as opposed to 3.5-4.5 b.y. based on earlier time scales and implies an anomalously high sea floor spreading rate.

Based on Montanari *et al.'s* (1985) time scale and extrapolation from sediment rate curves, the age of the North American microtektite horizon is about 35.9 ± 0.4 Ma. This age is in fair agreement with the new $^{40}Ar/^{39}Ar$ age of 35.4 ± 0.6 Ma from Barbados tektites (Glass *et al.*, in press) which are considered to come from the same

© Meteoritical Society • Provided by the NASA Astrophysics Data System

1987Metic..22...25K

source material as the North American tektites based on Nd and Sr isotopic composition (Ngo *et al.*, 1985). Glass *et al.* (in press) used this new $^{40}Ar/^{39}Ar$ date to estimate an age of 34.4 ± 0.6 Ma for the Eocene-Oligocene boundary. This age appears a little too young when compared with the Montanari *et al.* time scale.

$CaCO_3$ AND EXCESS Ir

Microspherule and microtektite layers are frequently associated with increased $CaCO_3$ dissolution apparent in poor faunal preservation and up to 50% reduction in carbonate. Some microspherule layers associated with strong $CaCO_3$ dissolution also show high Ir concentrations (Table 2). When Ir is ratioed to Al, however, the Ir peak all but disappears in some sections, as for example in Sites 462 and 612, indicating that the concentration is simply a function of the clay content. In other sections a significant excess of Ir remains when Ir is ratioed to Al as in Sites 292 and 315A indicating an abrupt increase in some form of supply. Thus, care must be taken to distinguish between an Ir excess due to an abrupt increase in the supply, and an apparent Ir excess due to concentration as a result of carbonate loss. Iridium analysis to date has revealed a major Ir concentration associated only with the crystal bearing microspherule layer. Both the North American microtektite layer and the *G. semiinvoluta* Zone microspherule layer appear to contain little excess Ir.

STRATIGRAPHY AND GEOCHEMISTRY

GLOBIGERAPSIS SEMIINVOLUTA ZONE MICROSPHERULE LAYER

The *Globigerapsis semiinvoluta* Zone microspherule layer is easily identified stratigraphically on the basis of planktonic foraminifers. This microspherule layer is closely associated with the global demise of the *Globigerapsis* group consisting of *G. semiinvoluta, G. howei, G. mexicana* and *G. index* (Keller, 1983, 1986a). These species dominate the *G. semiinvoluta* Zone interval up to the time of the microspherule horizon where they abruptly decline and shortly above this layer become extinct. Radiolarian stratigraphy at this interval is often not precise due to poor preservation or absence of siliceous microfossils. The *G. semiinvoluta* Zone microspherule layer has been found in the western equatorial Pacific (Site 292), eastern Indian Ocean (Site 216) and possibly in southern Spain (Fig. 1).

DSDP SITE 292: West Equatorial Pacific

DSDP Site 292 is located on the Ryuku Ridge in the western equatorial Pacific (Fig. 1). During the late Eocene the depth of deposition was about 1628 m and sedimentation was predominantly pelagic with about 80% carbonate consisting of calcareous tests of foraminifers and nannoplankton. The remaining 20% consist of biogenic silica (sponge spicules and radiolarian), intermittent volcanic ash layers, and clay. (The paleodepth was determined using the method of Sclater *et al.*, 1985.)

© Meteoritical Society • Provided by the NASA Astrophysics Data System

1987Metic..22...25K

Stratigraphy

Late Eocene sediment recovery during drilling of Site 292 was poor; except for core 36, only 1/3 to 1/2 (2-3 sections) of the core barrel length was recovered (Fig. 2). (Core barrel length is 9.5 m, divided into six sections of 1.5 m each plus the core catcher (cc).) Calcareous microfossils are abundant and generally well preserved except in short intervals where increased carbonate dissolution is noted in lower $CaCO_3$ and by breakage or absence of the solution prone delicate species *Globigerapsis semiinvoluta,* or where dissolution is severe, by absence of planktonic foraminifera. There is little evidence of older reworked sediments in this section.

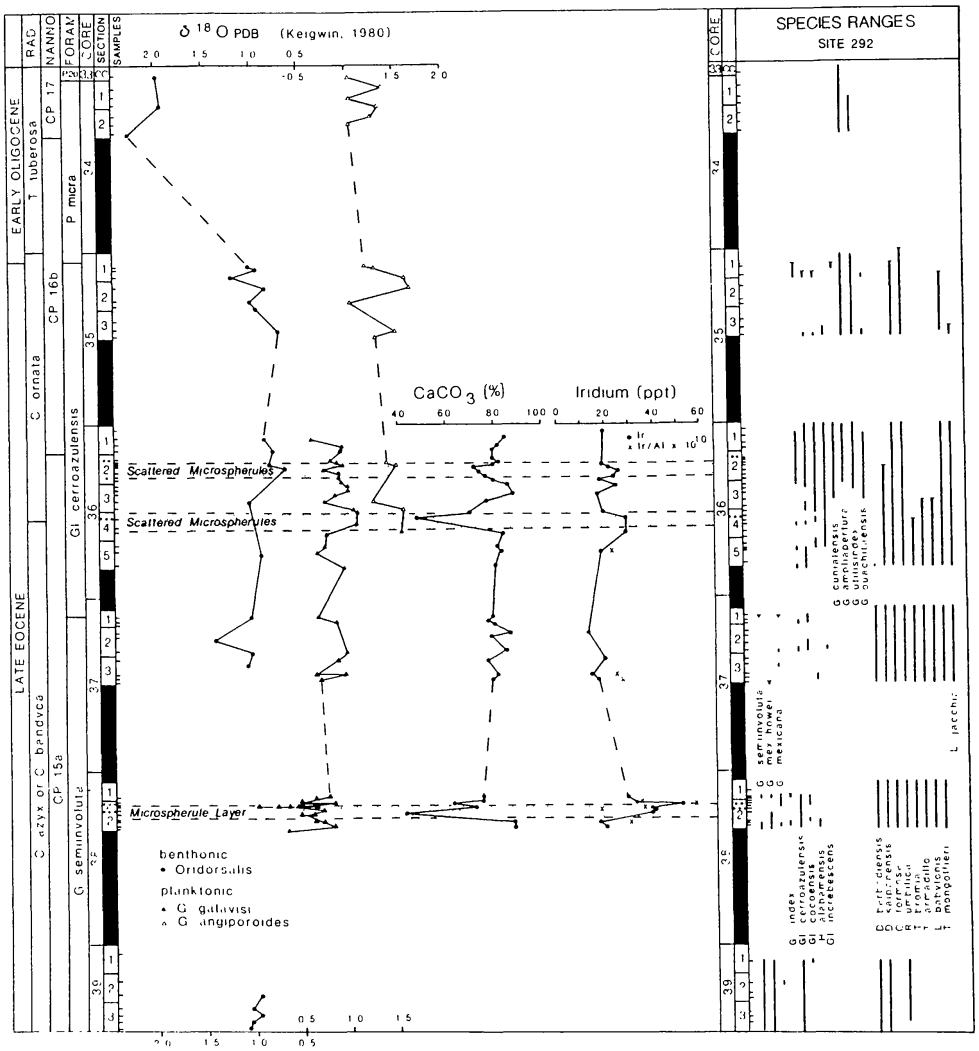

Fig. 2 DSDP Site 292: Ir, $CaCO_3$ (%), oxygen isotope data of benthonic and planktonic foraminifera, ranges of key stratigraphic species and stratigraphic position of microspherules plotted against core depth. Each core has six sections numbered 1 to 6, each section is 1.5 m long. Incomplete core recovery, which removes lower sections, is indicated by black intervals.

© Meteoritical Society • Provided by the NASA Astrophysics Data System

1987Metic..22...25K

Stratigraphic zonation is based primarily on planktonic foraminifera. The early Late Eocene *G. semiinvoluta* Zone is defined by the range (first and last appearance) of this species. In Site 292 the last appearance of *G. semiinvoluta* is observed in Core 37-1 (Fig. 2). Partly due to carbonate dissolution this species is rare above the microspherule layer in Core 38-2. Because carbonate dissolution is frequently observed in deep sea sediments in the upper part of the range of *G. semiinvoluta* (Keller, 1983, 1986a), there may be some uncertainty in the true extinction level above the microspherule layer in some sections studied.

The latest Eocene to the Eocene-Oligocene boundary is marked by the *Globorotalia cerroazulensis* Zone. This zone spans the interval from the *G. semiinvoluta* extinction to the extinction of the *Gl. cerroazulensis* group (three species) and the extinction of the genus *Hantkenina*. The extinction of these species defines the Eocene-Oligocene boundary and mark the fourth late Eocene stepwise extinction event. In Site 292 this extinction event occurs in Core 35-1 (Fig. 2). No microspherule layer has been found associated with this extinction event.

Nannofossil stratigraphy was found to be highly variable between sites and across ocean basins (Keller, 1986a; Molina *et al.*, in press), but is illustrated in Figure 2 for comparison. Late Eocene radiolarian stratigraphy based on subdivision of *Thyrsocyrtis bromia* Zone was found to correlate well with the planktonic foraminiferal zonation. Although radiolaria are generally rare in Site 292, the subzone *Calocyclas bandyca/ Cryptopora ornata* boundary could be interpreted from Ling's (1975) data as occurring in Core 36-4 coincident with an occurrence of microspherules. The stratigraphically useful species ranges of these three microfossil groups are illustrated in Figure 2.

Oxygen isotope values are illustrated for bottom water (benthonic foraminifer *Oridorsalis*) and surface water conditions (planktonic foraminifer *Globigerina galavisi* and *G. angiporoides*, Table 2, Fig. 2). Benthonic foraminifers indicate a major drop in oceanic bottom water temperature at the Eocene-Oligocene boundary. This cooling is observed worldwide and marks the development of the psychrosphere, or two layer ocean with cold bottom and warm surface water layers (Shackleton and Kennett, 1975; Keigwin, 1980). There is generally high variability in the planktonic foraminiferal oxygen isotope data through the Late Eocene, but no clear climatic trend is indicated. The 0.5 per mile fluctuations may be due to sample variability.

Microspherule Layers and Geochemical Data

A microspherule layer was found in Core 38 section 2 of Site 292 near the top of the *G. semiinvoluta* Zone (Keller *et al.*, 1983) and within the radiolarian *Calocyclas bandyca* or *C. azyx* Subzone. A search for the exact position of this layer in the unsampled archive core half located it between 75-80 cm of section 2 and scattered microspherules due to bioturbation were observed between 35 and 90 cm (Table 1). We found a total of 33 microspherules (in 5 cm^3 sediment) in this layer and Glass and co-workers (Glass *et al.*, 1985) reported a total of 102 microspherules. There is an iridium spike of 51 parts per trillion associated with this microspherule layer. This spike is also apparent when Ir is ratioed to Al and is therefore not an artifact of Ir concentration due to carbonate solution (Fig. 2).

Rare microspherules were also found in the *Globorotalia cerroazulensis* Zone in Core 36-4 (37-115 cm) at the *C. banyca/C. ornata* Subzone boundary and Core 36-2

© Meteoritical Society • Provided by the NASA Astrophysics Data System

1987Metic..22...25K

(70-130 cm) (Table 1, Fig. 2) as reported earlier by Glass and Crosbie (1982), Glass *et al.* (1985), and Keller *et al.* (1983). Microspherules found at the *C. banyca/C. ornata* Subzone boundary in deep-sea sections elsewhere have been identified as crystal bearing spherules (Maurasse and Glass, 1976). Iridium values associated with these two microspherule occurrences in Site 292 are 29 and 26 ppt respectively (Table 2, Fig. 2). Due to insufficient sediment for analysis, no Al data was obtained.

Carbonate values show two sharp drops from a high of 85% to a low of 40% in Cores 38-2 and 36-4, and a smaller decrease from 82% to 72% in Core 36-2 (Table 2, Fig. 2). This reduction in carbonate may be due to a sudden and temporary change in ocean surface fertility as a result of sea-level rise, or it may be impact related, as for instance a decrease in sunlight reaching the earth due to a dust cloud. A sudden temporary decrease in carbonate is associated with all late Eocene microspherule and microtektite layers observed to date.

The Core 36-4 and 36-2 microspherule occurrences are not well defined layers and Glass and co-workers (Glass *et al.*, 1985) consider them reworked from the older Core 38-2 layer in the *Globigerapsis semiinvoluta* Zone. Moreover, based on major element compositional analysis they consider the *G. semiinvoluta* Zone layer to be the same as the crystal bearing *Globorotalia cerroazulensis* Zone layer. We will show here that both stratigraphally and geochemically the Core 36 and Core 38 microspherules are distinctly different. However, we lack sufficient data to distinguish between the Core 36-2 and Core 36-4 microspherules.

We discussed above that stratigraphically Core 38-2 is in the uppermost *G. semiinvoluta* Zone and Core 36 is in the *Globorotalia cerroazulensis* Zone. These two zones are associated with very different faunal assemblages and no evidence of reworked *G. semiinvoluta* Zone fauna was found in Core 36. Furthermore, radiolarian stratigraphy places the Core 36 microspherules at or near the *C. bandyca/C. ornata* Subzone boundary (correlatable to *Gl. cerroazulensis* Zone) identifying them as both younger than Core 38-2 microspherules and coeval with the crystal bearing microspherules found elsewhere (Fig. 2). Therefore, stratigraphically Core 38-2 and Core 36 microspherule occurrences cannot be considered the same.

There is also a compositional difference in CaO and Al_2O_3 of SiO_2 equivalent microspherules of Core 36 and Core 38. In Figure 3, we have plotted compositional data from Glass (written communication, 1983), Glass *et al.* (1985) and D'Hondt *et al.* (1987). Firstly, there is no significant major element compositional difference apparent between glassy (microtektites) and crystal bearing microspherules (data from Glass *et al.*, 1985). This suggests that these two types of microspherules within the same layer have the same origin. Secondly, microspherules from Core 38-2 tend to be higher in CaO and lower in Al_2O_3 than SiO_2 equivalent microspherules from Core 36. This compositional difference suggests a different origin for the Core 36 and Core 38 microspherules.

© Meteoritical Society • Provided by the NASA Astrophysics Data System

1987Metic..22...25K

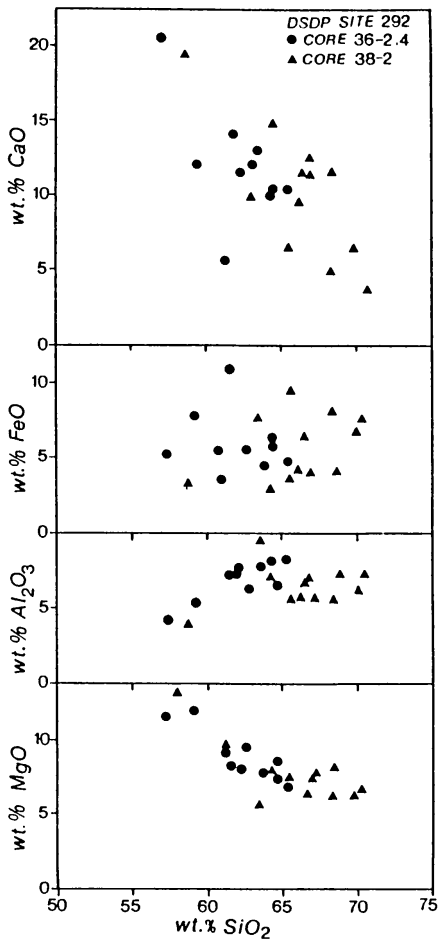

Fig. 3 Major oxide versus SiO_2 content for microspherules from DSDP Site 292 Core 36 and Core 38. Core 36 data from Glass *et al.* (1985) and Glass (written communication, 1983). Core 38-2 data from Glass *et al.* (1985) and D'Hondt *et al.* (1987).

Glass *et al.* (1985) argue for the same origin for the *G. semiinvoluta* Zone and the crystal bearing microspherule layers of the *Gl. cerroazulensis* Zone on the basis of his separation of microspherules of different layers and localities into glassy (microtektites by definition), crystal bearing and cryptocrystalline microspherules. However, his own data plotted in a ternary diagram shows a clear separation into three distinct and non-overlapping fields represented by the North American microtektite layer, the crystal bearing microspherule layer and the cryptocrystalline layer of the *G. semiinvoluta* Zone (Fig. 4). For instance, Site 292, Core 38-2 microspherules are significantly different from the crystal bearing microspherule layer in their percent abundance of microtektites, crystal bearing spherules and cryptocrystalline spherules. Only 18% of the microspherules in Core 38-2 contain crystals (cpx) as opposed to 68-72% in the crystal bearing microspherule layer and 65% are considered cryptocrystalline as opposed to 20-30%. In addition, 17% in Core 38-2 are microtektites (non-crystalline) whereas only 2-8% of the crystal bearing microspherule layer are microtektites.

© Meteoritical Society • Provided by the NASA Astrophysics Data System

1987Metic..22...25K

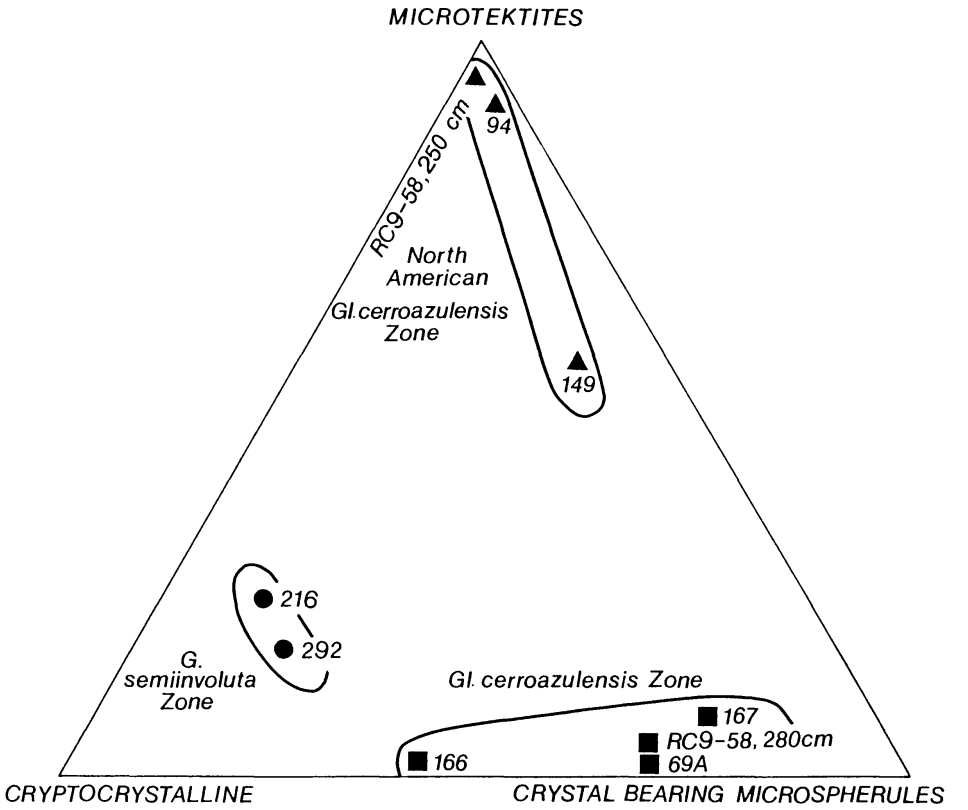

Fig. 4 Percentage of glassy microtektites, cryptocrystalline and crystal bearing microspherules from the North American microtektite layer, the crystal bearing microspherule layer and the *G. semiinvoluta* Zone layer plotted on a ternary diagram. Note these three layers occupy distinctly different and non-overlapping fields. Data from Glass *et al.* (1985).

Faunal Turnover

An expanded illustration of the faunal and geochemical parameters associated with the *Globigerapsis semiinvoluta* Zone microspherule layer of Site 292 is illustrated in Figure 5. The lowest carbonate values (40%) are directly associated with the microspherule layer, and increase to about 80% 35 cm above the layer. Iridium values show a broad concentration between 10 and 90 cm spanning the interval in which bioturbation and scattered microspherules were found. The *Globigerapsis* group consisting of four species dominates the fauna up to 68% relative to other species and catastrophically declines to 1% at the microspherule layer. Whether this decline occurred already in the 20 cm below the microspherule layer cannot be determined because this sample interval is depleted. There was an increase in the cooler water *Globigerina linaperta — G. angiporoides* group relative to all other species at this time which suggests a cooling trend. Oxygen isotope data of planktonic foraminifers provide no unequivocal climatic information; these data are highly variable even within the same samples probably due to vital effects.

© Meteoritical Society • Provided by the NASA Astrophysics Data System

1987Metic..22...25K

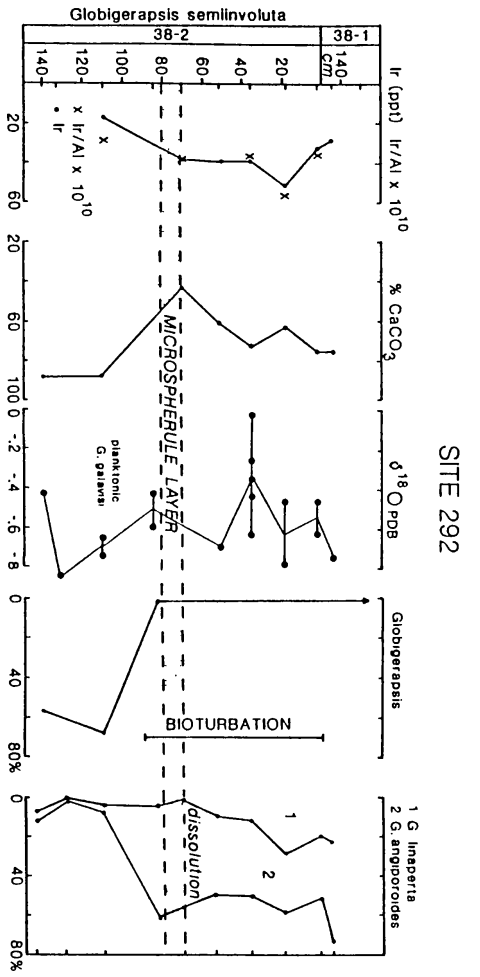

Fig. 5 DSDP Site 292: Expanded interval containing the *Globigerapsis semiinvoluta* Zone microspherule layer, Ir, $CaCO_3$, oxygen isotope data and relative abundances of dominant species plotted versus core depth. Note the decrease in $CaCO_3$, decline in the *Globigerapsis* species group to 1% and increase in the cooler water *Globigerina linaperta* and *G. angiporoides* at the microspherule layer. Due to sediment depletion of Core 38-2 between 85-105 cm, no samples are available from this critical interval.

In summary, our faunal, stratigraphic and major element compositional data as well as Glass *et al.'s* (1985) data show distinct differences between the Site 292, Core 38-2 and Core 36-2 microspherules as well as between Core 38-2 and microspherule layers of other localities indicating that they belong to different events.

DSDP SITE 216: Eastern Indian Ocean

DSDP Site 216, located in the eastern Indian Ocean was at a paleodepth of 1595 m during the late Eocene deposition of pelagic carbonate ooze (90-95%) consisting of calcareous nannofossils and foraminiferal shells. Planktonic foraminifers are well

© Meteoritical Society • Provided by the NASA Astrophysics Data System

1987Metic..22...25K

preserved, but curiously contain short intervals where nearly all shells are dissolved or broken as for instance immediately above the microspherule layer. Because of the shallow depth of deposition, fluctuation of the CCD is not a likely explanation for this dissolution (Fig. 6).

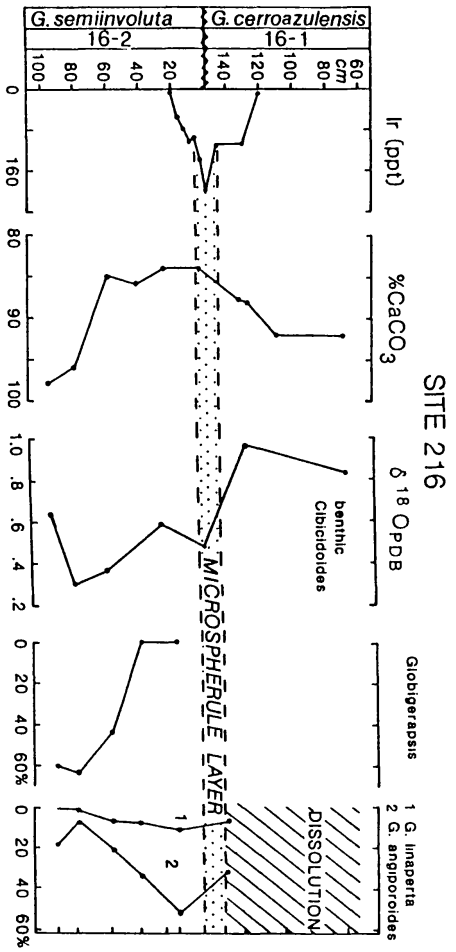

Fig. 6 **DSDP Site 216: *Globigerapsis semiinvoluta* Zone microspherule layer, Ir data from Asaro and Michel in Glass *et al.* (1985), $CaCO_3$, oxygen isotope data of benthonic foraminifera and relative abundances of dominant species plotted versus Core depth. Note wavy line between Core 16 section 2 and 1 indicates presence of a hiatus at the microspherule layer. The decrease in $CaCO_3$ and the relative abundance decline of the genus *Globigerapsis* 35 cm below the microspherule layer appears to be due to carbonate dissolution.**

A well defined microspherule layer is present in Core 16 between sections 1 and 2 (Table 1, Fig. 6). Stratigraphically section 2 is in the *G. semiinvoluta* Zone. A short hiatus, or period of nondeposition, appears to be present at this microspherule layer (Keller, 1986a). Iridium analysis by Asaro and Michel (in Glass *et al.*, 1985) shows

© Meteoritical Society • Provided by the NASA Astrophysics Data System

1987Metic..22...25K

a concentration spike of about 200 ppt at this interval (Fig. 6). A decrease in carbonate occurs 50 cm below the microtektite layer coincident with the catastrophic decline of the *Globigerapsis* group. The decline of this group prior to the microspherule layer appears to be due to carbonate dissolution rather than biologic causes. Calcareous shells of *Globigerapsis semiinvoluta* and *G. howei* are very delicate and more solution prone than other species. Planktonic foraminifers are also nearly completely dissolved in a 70 cm interval beginning just above the microspherule layer at 140 cm of Core 16-1 to 70 cm above (Fig. 6). This dissolution increase may indicate a change in fertility beginning at the microspherule layer and/or cooler more corrosive bottom water conditions. Oxygen isotope data of benthic foraminifera indeed suggest a cooling of bottom waters beginning at the microspherule layer (Fig. 6; Table 2) and a cooling trend is indicated through the late Eocene (Keigwin and Corliss, 1986).

The microspherule layer in Site 216 appears to be the same *G. semiinvoluta* Zone layer as observed in Site 292, although carbonate dissolution somewhat obscures the stratigraphic relationship. A strong similarity between these two layers is also evident in the data by Glass and co-workers (Glass *et al.*, 1985) who have differentiated between microtektites, crystal bearing and cryptocrystalline spherules. Their data shows a strong relationship between Site 292 and Site 216 microspherules with 17% and 24% microtektites, 18% and 14% crystal bearing spherules, and 65% and 64% cryptocrystalline spherules respectively (Fig. 4). This data very strongly supports a common origin for these layers and differentiates them from the crystal bearing microspherule layer in the *Gl. cerroazulensis* Zone.

The major element compositional data of these two sites is plotted in Figure 7 based on data from Glass *et al.* (1985) and D'Hondt *et al.* (1987). The two sites show complete overlap in all major element compositions and a similar high variability. This high variability characterizes the *G. semiinvoluta* Zone layer of DSDP Sites 292 and 216. In contrast, the North American microtektite layer and crystal bearing microspherule layer of the *Globorotalia cerroazulensis* Zone are compositionally more restricted.

Figure 8 shows the compositional data for Al_2O_3, FeO, MgO and CaO for the *Globigerapsis semiinvoluta* layer, the crystal bearing microspherule layer and the North American microtektite layer (data from D'Hondt *et al.*, 1987). The North American microtektite layer is generally higher in Al_2O_3 and lower in CaO than either the crystal bearing microspherule layer or the *G. semiinvoluta* Zone layer. The crystal bearing microspherules are also compositionally more restricted than the *G. semiinvoluta* Zone layer, but there is some overlap. For SiO_2 equivalent microspherules this layer is generally higher in Al_2O_3 than the *G. semiinvoluta* Zone layer, but lower than the North American microtektites. The composition of CaO is higher than the North American microtektites, but lower than the *G. semiinvoluta* Zone layer, and FeO is generally higher than in either the North American or *G. semiinvoluta* Zone layers (Fig. 8).

Based on the compositional data illustrated in Figures 7 and 8 as well as Glass *et al.'s* (1985) data shown in Figure 4 we conclude that the Site 216 and Site 292, Core 38-2 microspherule layers represent the same event, and that this event is different from those events which produced the crystal bearing microspherule layer and the North American microtektites.

© Meteoritical Society • Provided by the NASA Astrophysics Data System

1987Metic..22...25K

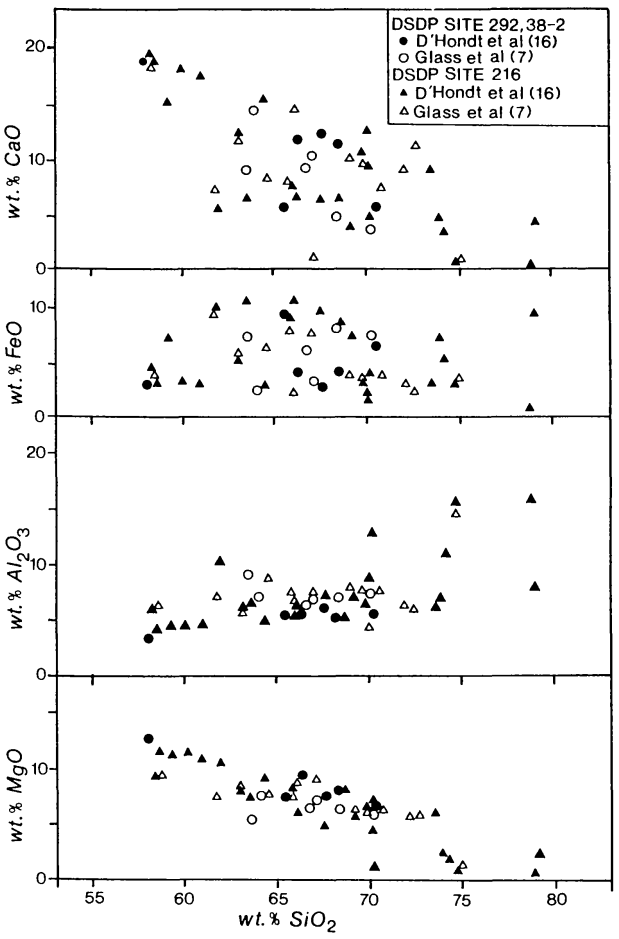

Fig. 7 **Major oxide versus SiO_2 content for microspherules from DSDP Sites 292 (Core 38-2) and 216 (Core 16-1/16-2). Data from Glass *et al.* (1985) and D'Hondt *et al.* (1987).**

© Meteoritical Society • Provided by the NASA Astrophysics Data System

1987Metic..22...25K

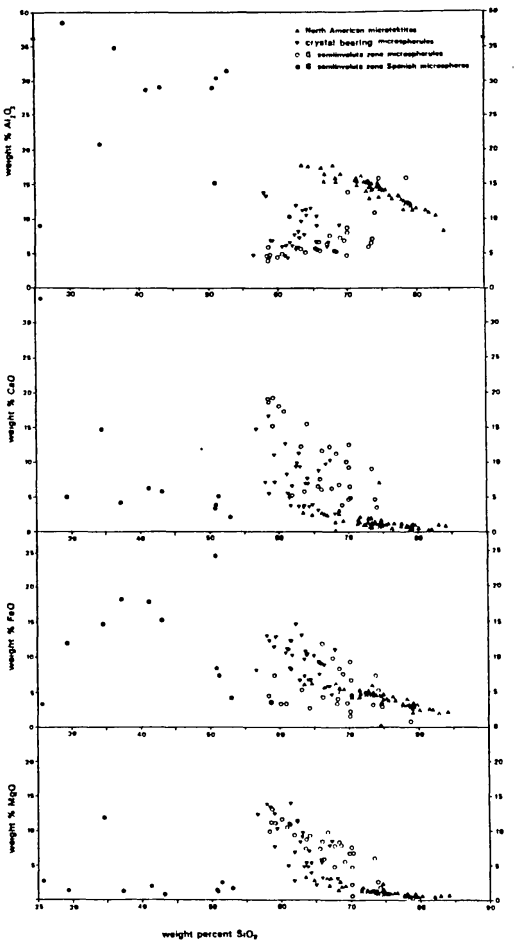

Fig. 8 Major oxide versus SiO_2 content for microspherules from the *G. semiinvoluta* Zone layer, the crystal bearing microspherules from the *Gl. cerroazulensis* Zone and the North American microtektite layer from the upper *Gl. cerroazulensis* Zone. All data from D'Hondt *et al.* (1987).

Molino de Cobo, Southern Spain

The Molino de Cobo section is part of the Cañada formation (Eocene to early Miocene age) of the Betic Cordillera of Andalucia, southern Spain. The Upper Eocene sequence is 68 m thick and consists of 30-90 cm thick beds of bioclastic calcarenites alternating with 1-5 m thick beds of grey-green marls. The calcarenites represent turbidite deposits with bioclasts of smaller and larger benthic foraminifera and calcareous algae of platform origin. Rare reworked middle Eocene foraminifers are present in some of the calcarenitic and marly beds. Deposition probably occurred in a basin near a slope and platform with periodic downslope transport.

Preservation of planktonic foraminiferas is generally good, but nannofossils are less well preserved. The lower 45 m of the Late Eocene section is of *Globigerapsis semiinvoluta* Zone age and the upper 23 m are of *Globorotalia cerroazulensis* Zone age (Fig. 9).

© Meteoritical Society • Provided by the NASA Astrophysics Data System

1987Metic..22...25K

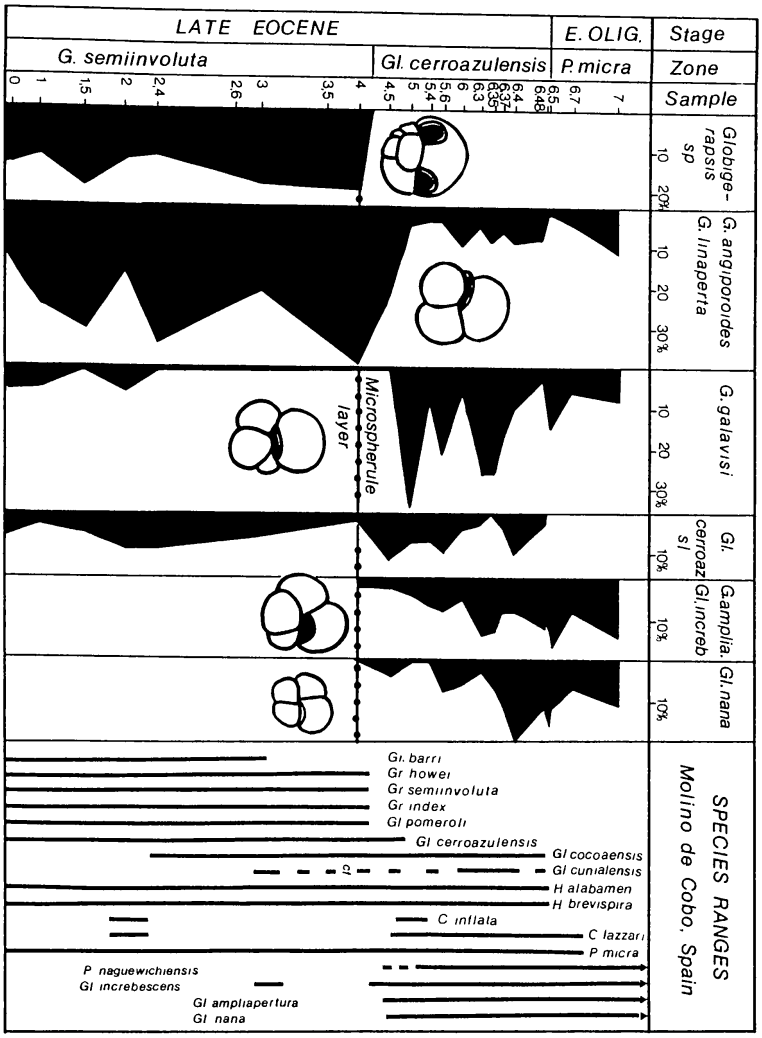

Fig. 9 Molino de Cobo, Spain: Relative abundances of dominant species, species extinctions and microspherules in the uppermost *G. semiinvoluta* Zone. Note the decrease in the *Globigerina* linaperta — *G. angiporoides* group, the increase in the cool water *Globigerina galavisi*, and the extinction of the *Globigerapsis* group at the microspherule layer.

Twenty-one microspherules have been found in a marly layer (sample 4, Fig. 9) which also contains well preserved *Globigerapsis semiinvoluta*, the index species that defines the *G. semiinvoluta* Zone. This sample also contains three other species of the *Globigerapsis* genus and their individuals reach 20% abundance of the total foraminiferal population. Only the cooler water species of the *Globigerapsis* group (*G. index*) survive for a short time above this interval. This implies that the *Globigerapsis* group became extinct at, or shortly after, deposition of the microspherule layer similar to Site 292. Also similar to Site 292 is the increased abundance (relative to other species) of the cool water species, *Globigerina galavisi* in Spain and *G. linaperta-G. angiporoides* group in Site 292; suggesting a climatic cooling. The fact that different

© Meteoritical Society • Provided by the NASA Astrophysics Data System

1987Metic..22...25K

cool water species are present in Spain and the northwest equatorial Pacific is a function of latitude. Based on these faunal data we conclude that stratigraphically the Site 292 and the Molino de Cobo microspherule layers represent the same time interval.

Nannofossil data also show a major decline and near extinction of two dominant species, *Discoaster barbadiensis* and *D. saipanensis,* at the microspherule layer (Molina *et al.*, in press). A similar faunal change in both foraminifers and nannofossils was also observed in the nearby coeval Fuente Caldera section (Perch-Nielsen, 1986) where no microspherules were found.

Faunal analysis of the Molina de Cobo section shows that the faunal turnover and species extinction event observed in Site 292, Core 38-2, and many other low latitude sections globally (Keller, 1983, 1986a) also affected middle latitudes and thus represents a major global event.

The glassy microspherules in the Molino de Cobo section physically resemble microtektites in shape, color, and surface morphology, but they show very little major element compositional overlap with other Late Eocene microtektites and crystal bearing microspherules. Figure 8 shows the major element chemical composition of the Spanish microspherules along with the *G. semiinvoluta* Zone layer from Sites 216 and 292, the North American microtektite layer and the crystal bearing microspherule layer (data from D'Hondt *et al.*, 1987). The Spanish microspherules are highly variable in SiO_2 ranging from 29% to 54%. They are higher in Al_2O_3 than any other microtektites or microspherules observed and also tend to be high in FeO and low in MgO and CaO. Some of the microspherules were found to contain inclusions of almost pure SiO_2.

Because of the anomalously high Al_2O_3 content we are not certain whether these microspherules are of impact origin. We have considered surface contamination from industrial sources, but find it unlikely because the section is about 70 km from the nearest city Granada. However, a train track runs along the outcrop and trains could possibly carry contaminants or produce slag from coal burning engines, although we know of no slag with such high Al_2O_3 content. We also consider surface contamination unlikely because in over 150 m of outcrop section collected, the microspherules were found only at the stratigraphic horizon containing the *Globigerapsis* extinction event. Thus, the anomalous chemical composition of the Molino de Cobo microspherules remains an enigma.

CRYSTAL-BEARING MICROSPHERULE LAYER: *GLOBORATALIA CERROAZULENSIS* ZONE

The crystal bearing microspherule layer of the *Globorotalia cerroazulensis* Zone is generally difficult to examine stratigraphically based on calcareous microfossils because of severe carbonate dissolution associated with this event. However, radiolarian stratigraphy places this microspherule layer near the *Calocyclas bandyca/Cryptopora ornata* Subzone boundary of the *Thyrsocyrtis bromia* Zone coincident with the extinction of five radiolarian species (Maurasse and Glass, 1976; Sanfilippo *et al.*, 1985).

Well defined layers of abundant crystal bearing microspherules up to 1400-2300 per gram sediments (Glass *et al.*, 1985), but generally in lower abundance (Table 1), are frequently observed in deep-sea sediments such as RC9-58 and DSDP Sites 69A, 70A, 65, 161A, 162 and 165 (Fig. 1). These microspherule layers have been described by Glass and coworkers (Glass *et al.*, 1985) as containing between 41% and 72% spherules with clinopyroxene crystals, 20% to 57% cryptocrystalline spherules and

© Meteoritical Society • Provided by the NASA Astrophysics Data System

1987Metic..22...25K

only 2-8% glassy spherules considered to be microtektites (Fig. 4). Microspherules from this layer are generally opaque brown, black, tan or yellow. They have generally higher concentrations of CaO and FeO and lower Al_2O_3 than SiO_2 equivalent North American microtektites. They are also generally higher in FeO and Al_2O_3 but lower in CaO than SiO_2 equivalent microspherules from the *G. semiinvoluta* Zone layer (Fig. 8). The crystal bearing microspherule layer is also associated with a significant Ir concentration spike whereas the earlier *G. semiinvoluta* Zone layer and the later North American microtektite layer are associated with little Ir excess.

In this section we discuss the new discoveries of probable crystal bearing microspherule layers in the central and West equatorial Pacific and the Ir spike of probably coeval age in the Bath Cliff section of Barbados.

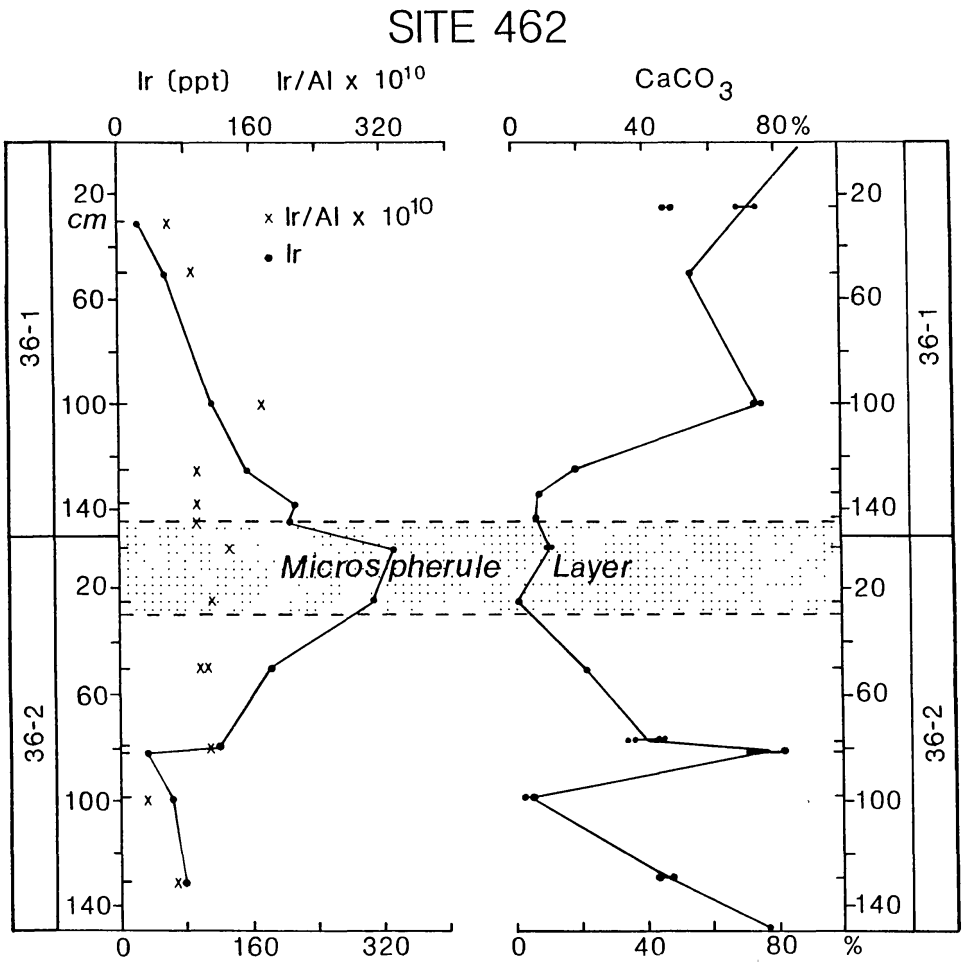

Fig. 10 DSDP Site 462: Ir and $CaCO_3$ analyses across the microspherule layer. Note Ir/Al ratio indicates that the excess Ir is primarily due to $CaCO_3$ dissolution.

© Meteoritical Society • Provided by the NASA Astrophysics Data System

1987Metic..22...25K

DSDP Site 462: West Equatorial Pacific

DSDP Site 462 is located in the west equatorial Pacific. Sediment deposition occurred at a paleodepth of 4880 m. Late Eocene sediments consist of mottled pale to brown nannofossil chalk with occasional interbeds of radiolaria. Carbonate ranges between 60-80%. Age control based on calcareous microfossils is poor due to severe carbonate dissolution and siliceous microfossils are rare. Reworked microfossils of middle Eocene age are commonly present.

A well defined layer with very abundant (> 1000) crystal bearing microspherules is present in Core 35 between sections 1 and 2. Examination of the archive cores shows the highest concentration of microspherules in a 12 cm interval spanning the bottom 5 cm of Core 36-1 to the upper 7 cm of Core 36-2. However, a sample at 27 cm in Core 36-2 also contained abundant microspherules and the layer is therefore considered spanning 32 cm (Fig. 10).

Carbonate dissolution is almost 100% at the microspherule layer and in one sample in Core 36-2 (97-99 cm) where only rare microspherules were found (Table 2). The Ir increases to about 320 ppt at the microspherule layer. But, when Ir is ratioed to Al, the Ir excess all but disappears (Fig. 10). Therefore, this Ir anomaly appears to be mainly an artifact of concentration due to carbonate dissolution.

Major element composition of Site 462 microspherules are plotted in Figure 8 along with crystal bearing microspherules from Sites 315A, RC9-58 and 69A (data from D'Hondt *et al.*, 1987). These microspherules including Site 462A have a similar major element composition characteristic of the crystal bearing microspherule layer described by Glass and co-workers (Glass *et al.*, 1985).

DSDP Site 315A: Central Equatorial Pacific

During the late Eocene sediment deposition in the central equatorial Pacific Site 315A occurred at about 3978 m depth. Late Eocene sediments consist primarily of light grey-green mottled nannofossil chalk and clay beds containing few calcareous (primarily benthic foraminifers and nannofossils) and siliceous microfossils (radiolaria). Stratigraphic control is poor.

A well defined microspherule layer was observed in the archive Core 10-6 between 33 and 47 cm (Fig. 11). This microspherule layer occurs just above the extinction of the radiolaria *T. tetracantha* and is nearly coincident with the NP20/21 nannofossil zone boundary which correlates to the uppermost part of the *Globorotalia cerroazulensis* Zone, just below the Eocene-Oligocene boundary. To determine the paleoclimatic conditions oxygen isotope analysis was done on the benthic foraminifer *Cibicidoides* (Fig. 9, Table 2). This species appears to have been partly recrystallized as observed in the 1 per mil lower values of this species as compared to coeval sample analysis at other locations (Keigwin and Corliss, 1986). Although recrystallization of foraminiferal tests precludes any conclusions regarding climatic changes at the time of the microspherule deposition, this magnitude of isotopic change is usually observed at the Eocene-Oligocene boundary. Thus, both nannofossil stratigraphy and stable isotopes suggest that this microspherule layer is very near the Eocene-Oligocene boundary. This may be due to a period of nondeposition following deposition of the microspherule layer. A period of nondeposition or increased carbonate solution following deposition of the microspherule layers has been observed in all geographic locations and in

© Meteoritical Society • Provided by the NASA Astrophysics Data System

1987Metic..22...25K

shallow or deep waters (Keller, 1986a). Carbonate values show no clear trends; they are generally low between 0-20%, but increase to a high of 40% in one sample above the microspherule layer (Fig. 11). An Ir spike of 250 ppt is observed in 10-6 (38-40) (Tables 1, 2) within the microspherule layer. The Ir/Al ratio which mirrors this spike, suggests that the Ir excess is not due to carbonate solution.

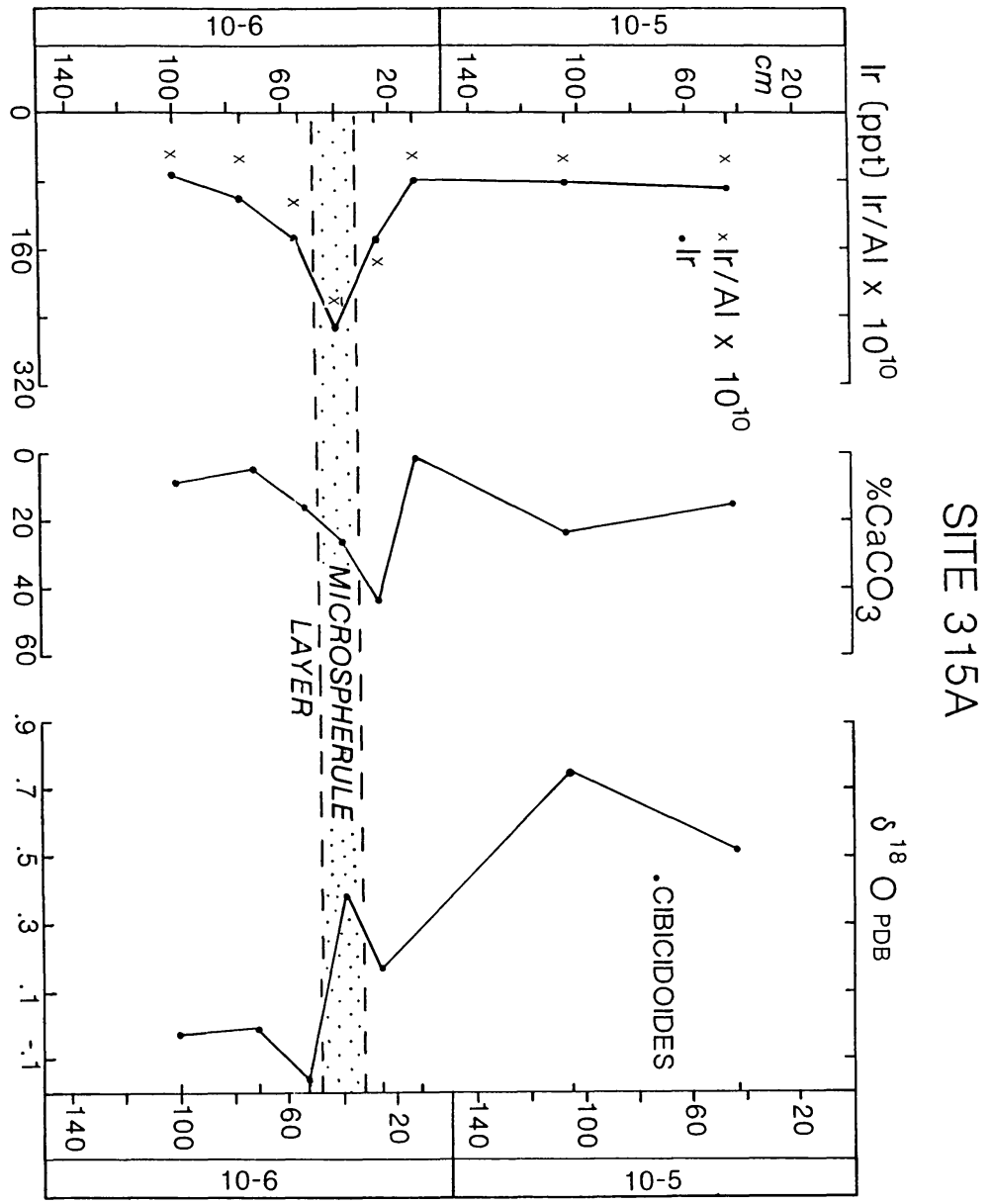

Fig. 11 DSDP Site 315A: Ir, $CaCO_3$ and oxygen isotope analyses of benthonic foraminifers across the microspherule horizon.

Over 174 microspherules greater than 63 μm were found in 2 cc of sediments in the Site 315A microspherule layer (Table 1). The major element composition of

© Meteoritical Society • Provided by the NASA Astrophysics Data System

1987Metic..22...25K

these microspherules is similar to those of Site 462 and other crystal bearing microspherules described by Glass *et al.* (1985) and D'Hondt *et al.* (1987). We therefore conclude that the Site 315 microspherule layer is part of the crystal bearing microspherule event.

Bath Cliff, Barbados — Ir spike

The stratigraphy of the Bath Cliff section on Barbados was earlier discussed in detail by Saunders *et al.* (1984) and Sanfilippo *et al.* (1985). The section was resampled by one of us (EMG) in contiguous samples, 5 cm long, across the microtektite layer and Ir anomaly and in contiguous 25 cm samples above and below this interval. We have analyzed the samples for Ir (Table 2) and searched the washed residue for microspherules. A well defined microtektite layer occurs in stratigraphic Zone *Globorotalia cerroazulensis* and a well defined Ir spike of 295 ppt occurs 25 cm below this layer in the lower part of this zone (Fig. 12). The Ir/Al ratio mirrors this Ir spike, indicating an increased source of iridium. Radiolarian stratigraphy places the *C. bandyca*/*C. ornata* Subzone boundary at the Ir spike (Sanfilippo *et al.*, 1985). This radiolarian subzone boundary is characterized by at least four species extinctions which coincide with the crystal bearing microspherule layer elsewhere (Maurasse and Glass, 1976) and is also usually accompanied by an Ir anomaly (Ganapathy, 1982; Glass *et al.*, 1985). The stratigraphic data suggests strongly that the Ir spike on Barbados represents the same event as the crystal bearing microspherule layer elsewhere.

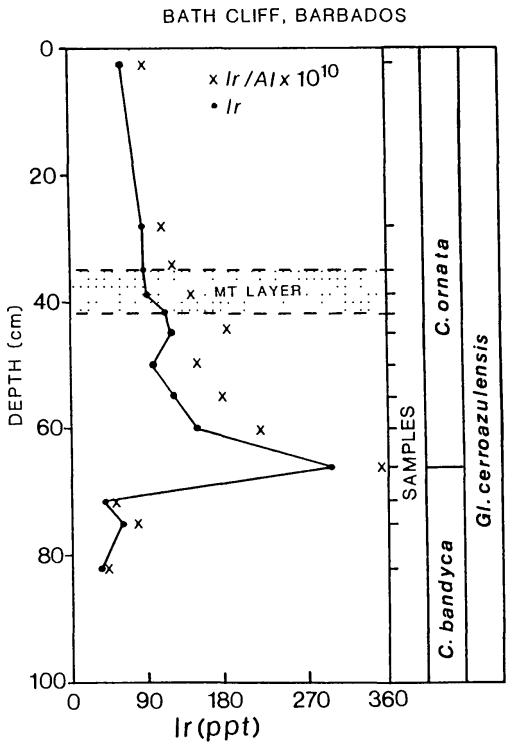

Fig. 12 Bath Cliff, Barbados: Ir profile and Ir/Al ratio across the microtektite layer. Note their spike occurs 25 cm below the microtektite layer.

© Meteoritical Society • Provided by the NASA Astrophysics Data System

1987Metic..22...25K

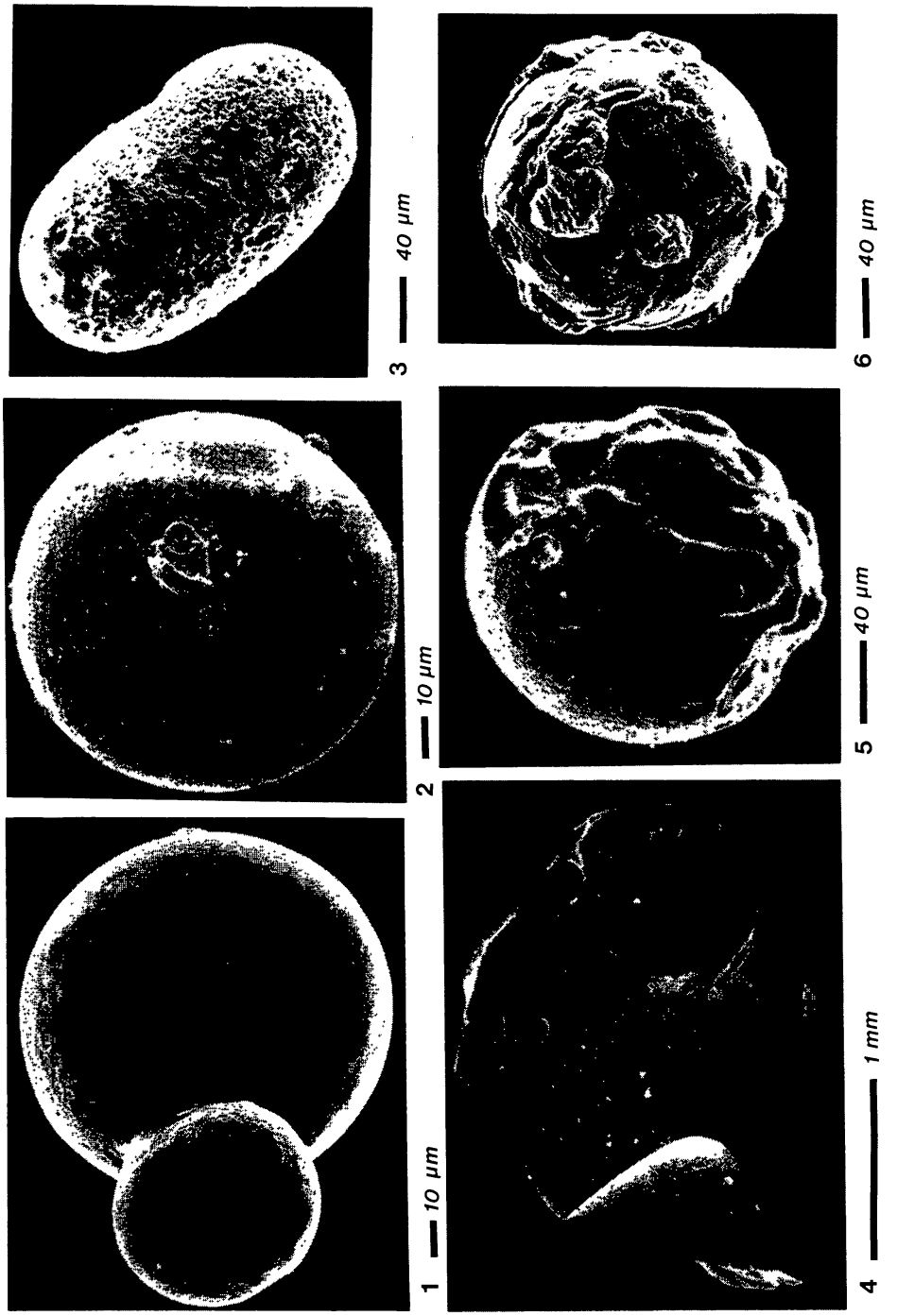

Plate 1 **Microtektites and Microspherules. 1) DSDP Site 292, Core 39-2, *G. semiinvoluta* Zone; 2) Molino de Cobo, Spain, sample 4, *G. semiinvoluta* Zone; 3,5) Bath Cliff, Barbados, *Gl. cerroazulensis* Zone; 3) corroded microspherule from the Ir spike, 5) partly dissolved spherule from the North American microtektite layer; 4,6) DSDP Site 612, Core 21-5 (115-117 cm), 4) microtektite fragment showing porosity, 6) microtektite encrusted with pyrite crystals.**

© Meteoritical Society • Provided by the NASA Astrophysics Data System

1987Metic..22...25K

We have carefully searched the sediment residue for microspherules through the Ir spike and found only a single corroded elongate microspherule (Plate 1) in the sample containing the maximum Ir-concentration. Energy dispersive x-ray analysis shows this microspherule to be higher in Ca than microtektites from the North American layer above. This suggests that microspherules may have been present originally and were subsequently dissolved. Although a single microspherule cannot provide convincing evidence of the presence of the crystal bearing microspherule layer, strong evidence is provided by its association with the Ir anomaly and the radiolarian extinctions that characterize this layer elsewhere.

NORTH AMERICAN MICROTEKTITE LAYER: *GLOBOROTALIA CERROAZULENSIS* ZONE

The youngest of the three late Eocene microspherule layers is characterized by over 90% glassy non-crystalline microtektites (Glass *et al.*, 1985). The microtektites have been shown to be compositionally similar to the North American tektites based on Rb/Sr and Sm/Nd data (Ngo *et al.*, 1985) and major oxide composition (Glass *et al.*, 1979, 1982, 1985; Sanfilippo *et al.*, 1985) and are therefore called North American microtektite layer. This layer has been found in the Caribbean, Gulf of Mexico and more recently off the Coast of New Jersey (Thein, in press; Keller, 1986a) (Fig. 1).

Stratigraphically the North American microtektite layer occurs in the *Globorotalia cerroazulensis* foraminiferal Zone near the first appearance of *Gl. cunialensis* and the first common *Globigerina ampliapertura* (Keller, 1986a). Based on radiolarian stratigraphy this layer occurs just above the *C. bandyca/C. ornata* Subzone boundary which marks the crystal bearing microspherule layer and Ir spike. In deep-sea sediments these two layers may be separated by as little as 25 cm. Within the stratigraphic resolution possible, these two events may be as little as a few thousand years to as much as a few tens of thousand or 100,000 years apart.

North American microtektites are physically and compositionally different from the two older layers; they frequently have etched or pitted surfaces due to solution (Plate 1) and are generally transparent colorless to yellow-brown. They are generally higher in SiO_2 than the two older microspherule layers and are also generally higher in Al_2O_3 and lower in CaO, FeO and MgO than SiO_2 equivalent microspherules of the other layers (Fig. 8) (Glass *et al.*, 1985; D'Hondt *et al.*, 1987).

Microtektites from the North American layer have been discussed in detail by Glass and Zwart (1979) and Glass *et al.* (1985). Therefore, in this paper we will discuss only our new analysis of the Barbados microtektites and the new discovery (Keller, 1986a; Thein, in press) at DSDP Site 612 off the coast of New Jersey.

Bath Cliff, Barbados: Microtektite Layer

The microtektite layer in the Bath Cliff section on Barbados is concentrated in a 10 cm layer located 25 cm above the Ir spike discussed earlier (Fig. 12). Three isolated microspherules with the same physical characteristics were found 20 cm above this layer and four were found 10 cm below this layer. These isolated microspherules probably represent bioturbation or contamination from the microtektite layer. The single corroded elongate microspherule from the Ir spike is different in physical appearance

© Meteoritical Society • Provided by the NASA Astrophysics Data System

1987Metic..22...25K

and major element composition as discussed earlier and is therefore not considered to be present as a result of reworking or contamination.

The microtektite layer appears to have little excess Ir, whereas the distinct Ir spike is 25 cm below (Fig. 12). Major element composition of these microtektites is illustrated in Figure 8 along with data from DSDP Site 612 and the upper microspherule layer in RC9-58 (data from D'Hondt *et al.*, 1987). Microspherules from all three localities have very similar compositions and clearly represent a common origin as also discussed by Glass *et al.* (1985) and D'Hondt *et al.* (1987). Sanfilippo *et al.* (1985) also showed that the Barbados microtektites are very similar in major element composition to the North American tektites and are therefore considered part of the North American strewn field.

DSDP Site 612, Northwest Atlantic

DSDP Site 612 is located off the coast of New Jersey near the Baltimore canyon. During the late Eocene deposition occurred at 690 m depth on the upper part of the slope off the continental shelf. Sediments consist of light grey siliceous carbonate ooze. Our preliminary analysis indicates approximately 40% carbonate, 20% biogenic silica and 40% clay. Microfossils are well preserved, but there are intervals with frequent reworked middle Eocene species.

A so far unique 2 cm thick microtektite debris layer was discovered in this northwest Atlantic Site 612 Core 21 section 5 between 115-117 cm (Keller, 1986a; Thein, in press). The largest microtektite fragments reach 2.5 cm in length and are very porous (Plate 1). Microspherules are also much larger, up to 2-3 mm in diameter, than usually observed, and are straw-yellow spherical or oblong similar to those found in the Barbados section. Very few small ($<$ 1 mm) microtektites were found which suggests size sorting probably due to winnowing. In the $>$ 63 micron fraction the 2 cm layer consists of 50% microtektite debris, 10-15% pyrite and $\sim$ 30% lithic fragments and about 7% carbonate. At the microtektite layer abundant reworked middle Eocene species of the *Globorotalia lehneri* Zone are mixed in with the latest Eocene *Globorotalia cerroazulensis* Zone fauna. Sediments below the microtektite layer are of middle Eocene *Gl. lehneri* Zone age and sediments above are of late Eocene *Gl. cerroazulensis* Zone age (Fig. 13). This indicates the presence of a hiatus at or below the microtektite layer. Based on planktonic foraminiferal analysis this microtektite layer occurs in the *Gl. cerroazulensis* Zone. Radiolarian stratigraphy places the sediments above the microtektite layers in the uppermost *C. bandyca* or lowermost *C. ornata* Subzones (Riedel, pers. comm., 1985) in close agreement with foraminiferal analysis.

The microtektites are physically and geochemically similar with those of the North American layer at Bath Cliff, Barbados, except for their larger size and slightly lower SiO_2 content. The SiO_2 value for the Barbados microtektites range between 72-82% whereas the Site 612 microtektites range between 70-75% (Fig. 8) (D'Hondt *et al.*, 1987).

An Ir spike of 115 ppt is present 15 cm above the microtektite layer, but when Ir is ratioed to Al, this spike disappears suggesting concentration of Ir due to dissolution (Fig. 12). This is also suggested by the severe carbonate dissolution between the microtektite layer and the Ir spike.

© Meteoritical Society • Provided by the NASA Astrophysics Data System

1987Metic..22...25K

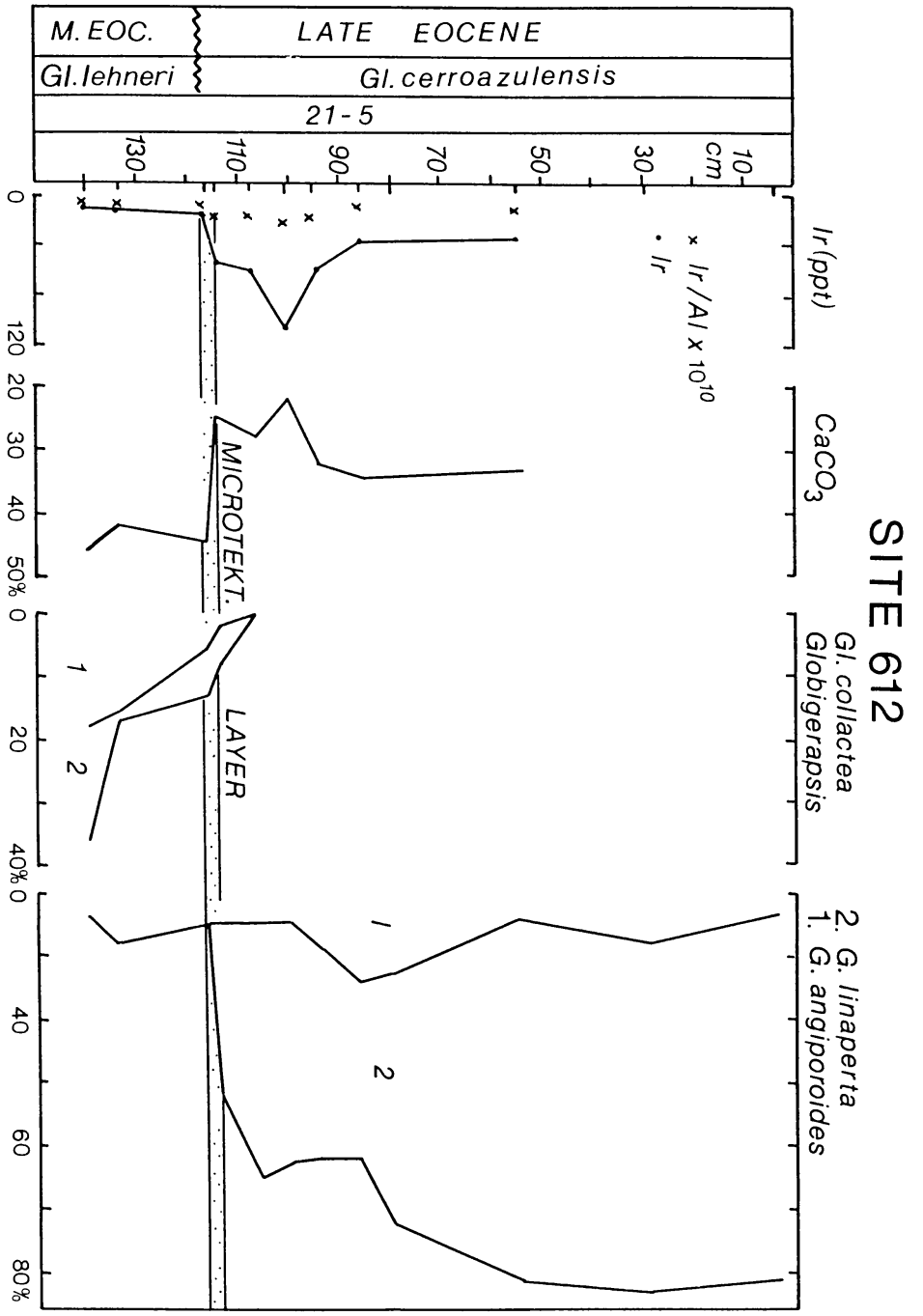

Fig. 13 **DSDP Site 612: Ir and $CaCO_3$ analysis and relative abundances of dominant species groups. Note the hiatus (wavy line) below the microtektite layer. Ir/Al ratio indicates that the Ir spike 20 cm above the microtektite layer is primarily a result of concentration due to carbonate dissolution. A low diversity, stressed cool water faunal assemblage is deposited above the microtektite layer.**

© Meteoritical Society • Provided by the NASA Astrophysics Data System

1987Metic..22...25K

Examination of other DSDP sites which contain the North American microtektite layer shows that no species go extinct at this time (Keller, 1983, 1986a). However, the faunal assemblages at DSDP Site 612 show a major decrease in diversity which was also observed in other localities. At Site 612 the faunal assemblage deposited during the first 28 cm, or a few thousand years following the impact event was of low diversity and, in addition, consisted primarily ($\sim$ 66%) of small dwarfed specimens of *G. linaperta*. Thereafter, these species resumed their normal size but also increased in abundance to $>$ 80% (Fig. 12). This suggests stressed conditions perhaps as a result of a fertility and nutrient change. No size analysis of foraminifers have been done at other locations. It is therefore unknown whether Site 612 represents a unique case. Locally different conditions in the off shore New Jersey Site 612 are, however, also indicated by the high abundance of pyrite (10-15%) mixed with the microtektite debris. In no other locality has such a high percentage of pyrite been observed. This pyrite suggests temporary reducing conditions possibly as a result of increased fertility and/or mass mortality of marine plankton at the time of the impact event.

IMPACT EVENTS AND EXTINCTIONS

Is there a relationship between impact related microtektite or microspherule layers and species extinctions? Four stepwise extinctions of planktonic foraminifers extended from late middle Eocene to the Eocene-Oligocene boundary and spanned the interval in which three microtektite and microspherule layers were deposited. No species extinctions of planktonic foraminifera precisely coincide with any of the three microspherule layers. Faunal assemblage changes, however, are associated with the *G. semiinvoluta* Zone layer and the North American layer and five radiolarian species extinctions coincide with the crystal bearing microspherule layer (Saunders *et al.*, 1984; Sanfilippo *et al.*, 1985).

The number of species extinctions and originations is not always the best indicator of the biotic response to environmental changes (Keller, 1986a). Species generally are rare in abundance as they originate and at the time of their extinction. Hence their final demise may be caused by minor ecological perturbations. A more accurate indicator of ecological success is population size, as measured by the number of specimens of a species relative to other species. When viewed in this context, deposition of each of the three Late Eocene microtektite and microspherule layers had a pronounced effect on planktonic organisms.

Although no species extinctions of marine plankton coincided precisely with the microspherule layer of the *G. semiinvoluta* Zone in marine plankton, there were major faunal abundance changes in both coccoliths and foraminifers. Species abundance data of planktonic foraminifers showed that the genus *Globigerapsis,* which at this time included four species, became nearly extinct at the time of the impact. At the west equatorial Pacific Site 292 this species group catastrophically declined from over 65% of the total population prior to the impact to 1% or less at the microspherule horizon (Figs. 2, 3) and became extinct shortly thereafter (Keller, 1986a). A similar dramatic and permanent reduction of this group was observed at the microspherule layer in the Molino de Cobo section of Spain (Fig. 9) and occurred globally at this time (Keller, 1983; 1986a, b). The ecologic niche vacated by the decline of this group was occupied by expanding populations of cooler water species.

© Meteoritical Society • Provided by the NASA Astrophysics Data System

1987Metic..22...25K

Coccolith species abundances are not routinely studied and their global population changes are less well known. Perch-Neilsen (1986) and Molina *et al.* (in press) reported major species abundance changes which occurred near the top of the *G. semiinvoluta* Zone microspherule layer in two sections of southern Spain (Molino de Cobo, and Fuente Caldera). In these sections two species, *Discoaster barbadsiensis* and *D. saipanensis,* decreased from about 50% of the total population to near extinction at the top of the *G. semiinvoluta* Zone.

Foraminiferal response to the impact event that produced the crystal bearing spherules of the *Gl. cerroazulensis* Zone is unclear because of severe carbonate dissolution in all sections studied. However, the extinction of five species of radiolaria occurs coincident with this microspherule layer and iridium anomaly globally (Saunders *et al.*, 1984; Sanfilippo *et al.*, 1985).

No species extinctions occurred among radiolaria or planktonic foraminifers at the time of the third impact event which produced the North American tektite and microtektite strewn field (Fig. 1), but there appears to have been a major effect on planktonic foraminiferal populations. At Site 612 off New Jersey, the impact event was accompanied by either a fertility change or mass mortality among the plankton, as indicated by abundant pyrite associated with the microtektites that probably was the result of a major influx of organic matter (dead plankton). Moreover, the indigenous cool water fauna exhibits the effects of stress at this time in the form of small dwarfed specimens of *Globigerina linaperta*. These pronounced size changes and abundance of pyrite have not been observed at other sites and may represent local environmental changes. However, a faunal turnover involving a change to cooler faunal assemblages at this time is observed globally (Keller, 1983, 1986a, b).

Thus, our data indicates that impacts may be related at least in part to some Late Eocene species extinctions and faunal assemblage changes. Among planktonic foraminifera the ecologically most sensitive and generally warmer water or surface dwelling species declined in abundance, or became extinct. This suggests climatic cooling. A Late Eocene climatic cooling trend is also indicated in the oxygen isotope record (Keigwin and Corliss, 1986). We have also observed that each of the microspherule and microtektite horizons is associated with increased carbonate dissolution. The low carbonate may be partly the result of decreased productivity related to sea level fluctuations (Keller *et al.*, in press), or to major impact events (Lewis *et al.*, 1982). However, it is very difficult to separate the effects of a productivity change from those of dissolution. Although the Late Eocene impact events appear to have had a measurably negative effect on marine plankton, the middle to Late Eocene stepwise mass extinction appears to have been the result of multiple causes, as there is no evidence of impacts associated with the two steps preceding or the step that followed the deposition of the presently known microspherule layers.

CONCLUSIONS

(1) There is very strong evidence in support of at least three microspherule layers in Late Eocene sediments in both stratigraphic and major element compositional data of microspherules. Our analysis shows that although there is major element compositional overlap between microspherules from the *G. semiinvoluta* Zone layer and the crystal bearing microspherules from the *Gl. cerroazulensis* Zone, and to

© Meteoritical Society • Provided by the NASA Astrophysics Data System

1987Metic..22...25K

a lesser extent between these two layers and the North American microtektite layer, each microspherule population has characteristic compositional features.

(2) The presence of probable crystal bearing microspherules in Site 292 (Core 36) extends this strewn field across the equatorial Pacific.

(3) Discovery of microtektites in the *Gl. cerroazulensis* Zone in Site 612 off New Jersey extends the North American strewn field from the Caribbean and Gulf of Mexico to the northwest Atlantic.

(4) Excess amounts of Ir can result from $CaCO_3$ solution as observed in two Sites 462 and 612. In such cases, when Ir is ratioed to Al, the Ir excess all but disappears.

(5) Strong $CaCO_3$ dissolution is associated with all late Eocene microspherule layers that were deposited in deep or shallow water. This increased carbonate solution may result from lower plankton productivity, or may have been caused by excess dust and water vapor in the atmosphere as a result of an impact.

(6) No planktonic foraminiferal species extinctions are directly associated with any of the three microspherule layers, but faunal assemblage changes are associated with both the *G. semiinvoluta* Zone and North American layers.

(7) Microspherules of the North American microtektite layer at Site 612, off New Jersey are associated with abundant pyrite and a dwarfed cool water fauna suggesting highly stressed environmental conditions and a sudden increase of organic matter (dead plankton) to the ocean floor.

(8) No unequivocal effect on climate at the times of the impact events was discerned in the stable isotope analysis of this study. The signal is largely obscured by vital effects and diagenesis. However, marine plankton indicate climatic cooling by the decline and ultimate demise of ecologically sensitive and generally warmer surface water species.

ACKNOWLEDGEMENTS

We would like to thank Dr. G.J. Wasserburg for review and helpful comments. We also thank Dr. B.P. Glass for constructive criticism, Dr. Bill Riedel for radiolarian analysis of DSDP Site 612, Drs. F. Asaro and H. Michel for the Ir data of DSDP Site 216, and Dr. L.D. Keigwin for stable isotope analysis of DSDP Sites 292 and 216. DSDP samples were made available by the National Science Foundation through the Deep Sea Drilling Project and Ocean Drilling Program. JSG and CJO thank the U.S. Department of Energy and the National Aeronautics and Space Administration (Planetary Materials and Geochemistry Program) for support. GK and EM thank the US-Spain Joint Committee for Scientific and Technical Cooperation for support.

REFERENCES

Berggren, W.A., D.V. Kent, and J.J. Flynn, 1985. Cenozoic geochronology. *Geol. Soc. Amer. Bull.* **96**, 1407-1418.

Ganatphy, R., 1982. Evidence for a major meteorite impact on the Earth 34 million years ago: Implications for Eocene extinctions. *Science* **216**, 885-886.

Glass, B.P. and J.R. Crosbie, 1982. Age of Eocene/Oligocene boundary based on extrapolation from North American microtektite layer. *Bull. Am. Assoc. Petrol. Geol.* **66**, 471-476.

© Meteoritical Society • Provided by the NASA Astrophysics Data System

1987Metic..22...25K

Glass, B.P. and M.J. Zwart, 1979. North American microtektites in Deep Sea Drilling Project cores from the Caribbean Sea and Gulf of Mexico. *Bull. Geol. Soc. Am.* **90**, 595-602.

Glass, B.P., C.A. Burns, J.R. Crosbie, and D.L. DuBois, 1985. Late Eocene North American Microtektites and Clinopyroxene Bearing Spherules. *Proc. of the 16th Lunar. Planet. Sci. Conf.*, part 1, *Journ. of Geophys. Res.* **90**, D175-D196.

Glass, B.P., D.L. DuBois, and R. Ganatphy, 1982. Relationship between an iridium anomaly and the North American microtektite layer in core RC9-58 from the Caribbean Sea. *J. Geophys. Res.* **87**, 425-428.

Glass, B.P., C.M. Hall, and D. York, 1986. $^{40}Ar/^{39}Ar$ Laser-probe Dating of North American Tektite Fragments from Barbados and the Age of the Eocene/Oligocene Boundary. *Chemical Geology* **59**, 181-186.

Glass, B.P., M.B. Swincki, and P.A. Zwart, 1979. Australasian, Ivory Coast, and North American tektite strewn fields: size, mass, and correlation with geomagnetic reversals and other earth events. *Proc. Lunar Planet Sci. Conf. 10th,* 2535-2545.

Harland, W.B., A.V. Cox, P.G. Llewellyn, C.A.G. Pickton, A.G. Smith, and R. Walters, 1982. A Geologic Time Scale. Cambridge Univ. Press, 131 pp.

D'Hondt, S.L., G. Keller, and R. Stallard, 1987. Major element compositional variation within and between different late Eocene microtektite strewn fields. *Meteoritics* **22**, 61-79.

Hut, P., W. Alvarez, W.P. Elder, T. Hansen, E.G. Kauffman, G. Keller, E.M. Shoemaker, and P. Weismann, in press. Comet Showers as possible causes of Stepwise Mass Extinctions. *Nature*.

Hsu, K.J., J. La Breque, S. Percival, R.C. Wright, A.M. Gombos, K. Pisciotto, P. Thucker, N. Peterson, J.A. McKenzie, H. Weissert, A.M. Karpoff, M.F. Carman Jr., and E. Schreiber, 1984. Numerical ages of Cenozoic biostratigraphic datum levels: Results of South Atlantic Leg 73 drilling. *Geol. Soc. Amer. Bull.* **95**, 863-876.

Kauffman, E.G., 1984. The Fabris of Cretaceous Marine Extinctions. In W.A. Berggren and J.A. Van Convering (eds.), Catastrophes and Earth History, Princeton Univ. Press, pp. 151-237.

Keigwin, L.D. Jr., 1980. Paleoceanographic change in the Pacific at the Eocene-Oligocene Boundary. *Nature* **287 (5784)**, 722-725.

Keigwin, L.D. and B.H. Corliss, 1986. Stable Isotopes in Late Eocene to Oligocene Foraminifera. *Geol. Soc. Amer. Bull.* **97**, 335-345.

Keller, G., 1983. Biochronology and Paleoclimatic implications of middle Eocene to Oligocene planktonic foraminiferal faunas. *Marine Micropaleontology* **7**, 464-486.

Keller, G., 1985. Eocene and Oligocene Stratigraphy and erosional unconformities in the Gulf of Mexico and Gulf Coast. *Jour. Paleo.* **59(4)**, 882-903.

Keller, G., 1986a. Stepwise mass extinctions and impact events: Late Eocene to early Oligocene. *Marine Micropaleontology* **10**, 267-293.

Keller, G., 1986b. Late Eocene impact events and stepwise mass extinctions. In Terminal Eocene Events, Ch. Pomerol and I. Premoli-Silva, eds., Elsevier Amsterdam, 403-413.

© Meteoritical Society • Provided by the NASA Astrophysics Data System

1987Metic..22...25K

Keller, G., S. D'Hondt, and T.L. Vallier, 1983. Multiple microtektite horizons in upper Eocene marine sediments: No evidence for mass extinctions. *Science* **221**, 150-152.

Keller, G., T. Herbert, R. Dorsey, S. D'Hondt, M. Johnsson, and W.R. Chi, in press. Global distribution of late Paleogene hiatus. *Geology.*

King, E.A., 1977. The origin of tektites: A brief review. *Am. Sci.* **64**, 212-218.

Lewis, J.S., G.H. Watkins, H. Hartman, and R.G. Priun, 1982. Chemical consequences of major impact events on Earth. In Geological Implications of Impacts of Large Asteroids and Comets on the Earth, L.T. Silver and P.H. Schultz, eds. *Geol. Soc. Amer. Special paper* **190**, 215-222.

Ling, H.Y., 1975. Radiolaria: Leg 31 of the Deep Sea Drilling Project. In *Initial Reports of the Deep Sea Drilling Project* **31**, 703-778.

Lowrie, W., W. Alvarez, G. Napoleone, K. Perch-Nielsen, I. Premoli Silva, and M. Toumarkine, 1982. Paleogene magnetic stratigraphy in Umbrian pelagic carbonate rocks: The Contessa sections. *Gubbio. Geol. Soc. Amer. Bull.* **93**, 414-432.

Maurasse, F. and B.P. Glass, 1976. Radiolarian stratigraphy and North American microtektites in Caribbean Core RC9-58: implications concerning Late Eocene radiolarian chronology and the age of the Eocene-Oligocene boundary: 7th Caribbean Geol. Conf. Proc., July 1974, Guadeloupe, pp. 205-212.

Molina, E., G. Keller, and E. Madile, in press. Late Eocene-Oligocene Stratigraphy of the Molino de Cobo section, Betic Cordillera, Spain. *Rev. Micropaleontologia España.*

Montanari, A., R. Drake, D.M. Bice, W. Alvarez, and H. Curtis, 1985. Radiometric time scale for the upper Eocene and Oligocene based on K/Ar and Rb/Sr dating of volcanic biotites from the pelagic sequence of Gubbio, Italy. *Geology* **13**, 596-599.

Ness, G., S. Levi, and R. Couch, 1980. Marine magnetic anomaly timescales for the Cenozoic and Late Cretaceous: A precis, critique and synthesis. *Reviews of Geophysics and Space Physics* **18**, 753-770.

Ngo, H.H., G.J. Wasserburg, and B.P. Glass, 1985. Nd and Sr isotopic composition of tektite material from Barbados and their relationship to North American tektites. *Geochim. Cosmochim. Acta* **49**, 1429-1485.

Orth, C.J., J.S. Gilmore, J.D. Knight, C.L. Pillmore, R.H. Tschudy, and J.S. Fassett, 1982. *Geol. Soc. Am. Spec. Paper* **190**, 423-433.

Perch-Neilsen, K., 1986. Calcareous Nannofossil Events at the Eocene/Oligocene Boundary. In Terminal Eocene Events, Ch. Pomerol and I. Premoli-Silva, eds. Elsevier Amsterdam, 275-282.

Raup, D. and J. Sepkoski, 1984. Periodicity of extinctions in the Geologic Past. *Proc. Natl. Acad. Sci. U.S.A.* **81**, 801-805.

Sanfilippo, A., W.R. Riedel, B.P. Glass, and F.T. Kyte, 1985. Late Eocene microtektites and radiolarian extinctions on Barbados. *Nature* **314 (6012)**, 613-615.

Saunders, J.B., D. Bernoulli, E. Muller-Merz, H. Oberhansli, K. Perch-Neilsen, W.R. Riedel, A. Sanfilippo, and R. Torrini, Jr., 1984. Stratigraphy of the Late Middle Eocene to early Oligocene in the Bath Cliff Section, Barbados, West Indies. *Micropaleontology* **30**, 390-425.

© Meteoritical Society • Provided by the NASA Astrophysics Data System

1987Metic..22...25K

Schackleton, N.J. and J.P. Kennett, 1976. Paleotemperature History of the Cenozoic and the initiation of Antarctic glaciation: oxygen and carbon isotope analyses in DSDP Sites 277, 279 and 281. In *Initial Reports of the Deep Sea Drilling Project* **29**, 743-755.

Sclater, J.G., L. Meinke, A. Bennett, and C. Murphy, 1985. The depth of the Ocean through the Neogene. In J.P. Kennett (ed.), The Miocene Ocean. *Geol. Soc. Memoir* **163**, 1-20.

Taylor, S.R., 1973. Tektites: a post-Apollo view. *Earth Sci. Rev.*, 101-103.

Thein, J., in press. A tektite layer at the Middle/Upper Eocene boundary on the New Jersey Continental Slope (Leg 95, Site 612). In Initial Reports of the Deep Sea Drilling Project, Leg 95, in press.

Manuscript received 7/11/86

© Meteoritical Society • Provided by the NASA Astrophysics Data System